Shock and Vibration 10 (2003) 231–267
IOS Press

A new simulation method providing shock mount selection assurance

Michael A. Talley[a,*] and Shahram Sarkani[b]
[a]*The George Washington University, Washington, D.C. 20052, USA*
[b]*The George Washington University, Washington, D.C. 20052, USA*

Received 1 November 2002
Revised 12 March 2003

Abstract. This paper presents the development and assessment of a practical and efficient process for assessing and/or designing shock isolation systems. This process combines practical methods for determining relative displacements and accelerations (e.g. shock response spectrum analysis) with a new, efficient, easy to use, 6 degree of freedom (6DOF) simulation method known as Shock Isolation Mount Predictions & Loading Estimates (SIMPLE). SIMPLE is also a tool that can easily account for uncertainties in isolated systems and their environments. The implementation of 6DOF rigid body theory in SIMPLE is validated by comparing simulation results with other analytical methods. This paper also summarizes assessments and designs for 60 different mounting systems using SIMPLE. In addition, experimental results from shock tests are compared with pre-test SIMPLE sensitivity simulations and with results of post-test model calibrations. These comparisons show the validity of: 1) using 6DOF analysis; 2) using statically derived load-deflection data for simulations; and 3) assessing and designing isolated systems using uncertainties in model parameters.

1. Introduction

1.1. Motivation and scope

There is an increased [1] reliance on isolation technology to protect mission critical, fragile, and sensitive components from the effects of shock and vibration. As a result, many equipment integrators, having no prior experience with shock-mounted systems, are in the position of having to make mount selections that will enable a system to pass shock and vibration qualification tests. The desire is to obtain validation and assurance that shock and vibration mounts are properly selected for the equipment racks, consoles, cabinets, and other structures being promoted. In many cases, equipment integrators rely on mount vendors and consultants for proposals and recommendations.

In general, the variety and frequency of applications for shock mounts is increasing. An example is rapid infusion of commercial off the shelf (COTS) items and newly developed technologies into shipboard environments. At this stage of product development, design time for isolated systems is short. Inefficient and inadequate analysis methods do not permit sufficient time to do trade studies. In practice, biased [2] or inefficient estimates of model parameters are often used because of the ease with which some of them can be obtained. An example is the use of statically derived load deflection curves when dynamic curves are not available. In addition, uncertainties in the structural, inertial and mount properties of the system as well as use of incorrect shock inputs for analysis result in improperly designed isolation systems. Time to perform investigations [3–6] to reduce these uncertainties may not be available. Therefore, the need exists to provide practical, efficient, and easy to use methods to rapidly assess the performance of shock and vibration mounted systems using available model parameters.

*Corresponding author. E-mail: m.a.talley@larc.nasa.gov.

ISSN 1070-9622/03/$8.00

1.2. Hypotheses

The hypotheses tested in this paper are: 1) Six degree of freedom simulation methods can be made practical, efficient, and easy to use by simplifying the specification and implementation of the many parameters used in analyzing isolated systems and 2) reasonable response predictions for isolated systems can be made even in the presence of uncertainties. People who will benefit are: mount vendors, equipment integrators, engineers, program managers, shock and vibration analysts, teachers, students, and the general public.

To test these hypotheses, a new efficient, easy to use 6 degree of freedom (6DOF) simulation method called Shock Isolation Mount Predictions & Loading Estimates [8] (SIMPLE) was developed and its use evaluated. SIMPLE specifically addresses the need for practicality and efficiency by providing: 1) estimates of the excursion space needed for dynamic travel of mounted systems; 2) rapid prediction of responses such as acceleration, velocity, force, displacement, etc.; 3) a design tool for the location, sizing, and orientation of mounts for equipment and structures; 4) calibration via optimization; 5) multivariate sensitivity analyses of system parameters; 6) a shock mount library of more than 250 mounts; 7) inputs from floating shock platforms, deck simulators; medium weight shock test machines, etc.; and 8) immediate presentation of data after simulation. What is not covered by the SIMPLE method is the application of dynamic vibration (or shock) absorbers [15] for multi-body systems.

1.3. Questions

Several questions arise regarding the use of SIMPLE as a simulation method for assessing shock and vibration problems:

1) What kind of simplifications can be made to make the simulation method efficient and easy to use?
2) What advantage does SIMPLE have over other analysis methods?
3) How sensitive are response predictions to model parameters such as those that characterize the mounts, their location, and the inertial properties of the rigid body?
4) What is the validity of SIMPLE response predictions when simulating with multi-axis inputs from deck simulator fixtures (DSFs); floating shock platforms (FSPs), medium weight shock machines (MWSMs) and others?

1.4. Research approach

First, a process for selecting and designing mounting systems was formulated to provide the context in which a simulation method like SIMPLE would be used. This process is described in the next section. Next, a review of literature was done to address the extent in which the questions have been answered. Based on the review and context of use for 6DOF methods supporting test planning, a theoretical basis for the SIMPLE simulation method was developed. Next, validation of SIMPLE predictions by benchmarking with other analytical methods was accomplished. Then, application of SIMPLE to provide actual assessments and designs for mounting systems was performed. These applications provided rapid assessments and designs (including simulations) for over 60 different mounting systems for the Navy Smartship Integrated Ship Controls System for CG 47 Class ships. The applications included: 1) an assessment of existing wire rope mount systems for cabinets on two CG 47 Class Smartships; 2) a mount performance trade study with different mounting options for each of these cabinets; and 3) determination of excursion space and acceleration levels for each mounting system selected for testing. Finally, test results were analyzed to test the validity of: 1) including 6DOF analyses in the assessment of coupled modes; 2) using statically derived load-deflection data for simulations; and 3) assessing and designing isolated systems using uncertainties in model parameters. Also, post-test model optimizations were performed on an isolated cabinet to test the limitations of the calibration process and the rigid body template used in SIMPLE.

1.5. Process used for selecting mounts

Specifying or estimating the shock environment is necessary for the assessment and/or design of shock isolation systems. The 3 most [10] popular methods of specification are: pulse shock, velocity shock, and shock response spectrum. Of these, the shock response spectrum (SRS) is the most representative of the real world. For this reason, the SRS is selected to begin the process for assessing and/or designing the shock isolation systems as shown in Fig. 1. The process is divided into two phases: 1) analysis using the classic [7] SRS or other methods and 2) assessment, confirmation, iteration or comparison of designs using the SIMPLE simulation method. The SRS is calculated and graphed using test input data measured at the equipment foundation and estimates of the damping of the

mount and system. Test input data may be acceleration time histories from floating shock platforms, deck simulator fixtures, drop tests, and other sources that include the effects of [13,16] dynamic foundation interaction or that may be approximated [11] as having infinite impedance. Damping may originate from the mounts as [16] well as the test fixture. Once the SRS is produced, system assessment or design follows. The simulation phase begins if the SRS analysis is considered to be insufficient.

For system assessment, the natural frequency of the isolated system in the direction of the input is determined. The SRS is then examined at that frequency to get an estimate of the system response. A comparison is made of the estimated response with the mount and systems properties. This involves comparing the amount of stroke available in the mount to the relative displacement required by the system. Also, a comparison may be made of the spectrum's acceleration level and velocity (at the mount system frequency) with equipment fragility requirements and other input limitations. Since SRS analyses are for simple one degree of freedom dynamic linear systems, the addition of relative displacements from equilibrium offsets and estimated rotations is necessary. SRS from rotational data may provide an estimate of the angular displacement, which could then be ultimately used to calculate the added relative displacement associated with rotation. However, this requires determination of rotational frequencies, calculations of mass moments of inertia, and access to the rotational data. A more practical and reliable method of assessing the rotations and coupled responses from multiple inputs is to perform a 6DOF simulation of the isolated system.

For system design, the SRS is examined to select acceptable natural frequencies for the isolation system. Based on these frequencies, mounts and the orientation of their principal axes on the cabinet are determined using the system weight and stiffness values derived from the mount force-deflection curves. Mounts are then configured to accommodate foundation and cabinet interfaces and minimize moments by keeping the system at least statically [10] balanced. An SRS analysis may not be sufficient when comparing different mounting options and their configurations. To minimize risk and have assurance of isolation system designs, a 6DOF simulation should be performed.

1.6. Contribution of research

1.6.1. New or improved methodology

This research improved the methods for assessing and designing isolated systems. It combined the classic SRS analysis and other existing methods with a new practical and efficient 6DOF simulation method. This new method takes complex and significant computational problems and provides comprehensive solutions in a practical and efficient manner. It provides a template for modeling isolated systems as 6DOF rigid bodies. The template can be changed as necessary to assess, confirm, iterate, and compare designs (e.g. trade studies). This includes selection of mounts from a library to save time when specifying mount properties. In addition, variances can easily be assigned to model parameters and sensitivity analyses run. Calibration of model parameters with measured data can also be performed.

No special knowledge is required to use the new simulation method and no overcomplicated modeling assumptions are necessary to obtain reasonable estimates of isolated system responses. For example, most 6DOF analysis tools such as finite element codes and specialized simulation tools require an extensive working knowledge and expertise to build and simulate models for shock isolated systems. Calibrating and implementing multivariate and univarite sensitivity analyses with such tools would be even more complicated and time consuming.

The validity of the new method was demonstrated by applying it to provide rapid assessments and designs for over 60 different mounting systems for the Integrated Ship Controls (ISC). The applications included: 1) an assessment of 14 existing wire rope mount systems for cabinets on CG 47 Class Smartships; 2) a mount performance trade study with 4 different mounting options for these cabinets; and 3) determination of excursion space and acceleration levels for each mounting system selected for testing. Using the mounting systems designed by the new method contributed significantly to qualification of the tested cabinets, all of which were successfully shock qualified and installed aboard ship.

The new 6DOF simulation method enables practical and efficient analyses of coupled mode responses of isolated systems. This is an improvement over other practical methods where uncoupled modes form the basis of analysis. These include: hand calculations; shock response spectra; mount sizing nomographs, tables, & charts; and other mount application tools that leave out rotational effects. The new 6DOF simulation method improves the efficiency in performing analyses of rigid body systems without loss of accuracy. This is possible due to intricate mathematical modeling of the complex dynamics of what appears on the surface to be a simple system (e.g. a rigid cabinet supported

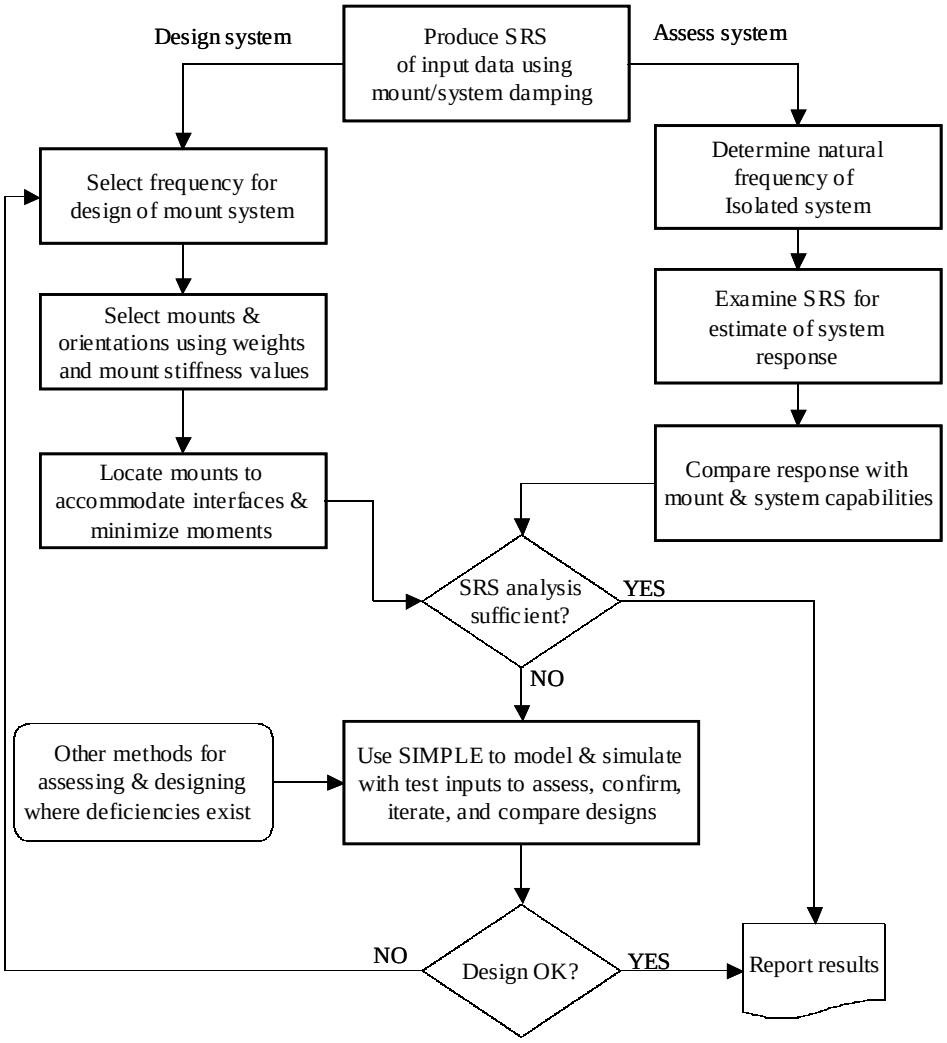

Fig. 1. Mount selection process.

by a set of mounts). In reality this system is quite complex. Two sample problems used to benchmark accuracy showed differences of less than 1% between the new simulation method and results of other 6DOF computer model calculations. The first problem validated the capability to predict the coupled modes of a rigid body and effects from damping. The second problem validated the capability to predict responses from a coupled mode system having multiple inputs.

1.6.2. New evidence

This research provides new evidence that reasonable response predictions for isolated systems can be made even in the presence of many uncertainties. Results of multivariate 6DOF sensitivity simulations, where 30 model parameters were randomly varied, were compared to experimental data. Comparisons showed that experimental results were within the 95% confidence bounds of the sensitivity results. This evidence shows the validity of: 1) using 6DOF analysis; 2) using statically derived load-deflection data for simulations; and 3) assessing and designing isolated systems using uncertainties in model parameters.

2. Literature review

2.1. Simplification to rigid body

In addressing question 1, the most obvious simplification is to consider the isolated cabinet or structure to be a rigid body. According to Racca [9], rigid body

analysis is applicable where the foundation and isolated structure is at least 10 times stiffer than the mount. This applies to many shock isolation systems, especially those for [5,10] electronic equipment on ships and submarines. The 10:1 stiffness ratio assures that at least 90% of the isolation is from the mounts and 10% is from the structure. The resulting ratio of structure to mount system natural frequencies is 3.2:1.0. A theoretical and experimental comparative study presented by Crede and Ruzicka [11] also suggests that rigid body theory is useful for mount system frequencies that are lower than the lowest natural frequency within the isolated structure. Structure to mount system frequency ratios of 2:1, 5:1, and 10:1 were compared. This study showed that for a structure to mount system frequency ratio of 5:1 or higher, rigid body theory produces accurate results as long as the structure to forcing frequency ratio is $>= 2:1$. For example, consider a cabinet approximated as a rigid body with a 7 Hz mount system that is to be tested on a 14 Hz deck. According to Crede and Ruzicka, rigid body analysis will produce accurate results when the natural frequencies of the mounted structure are $>= 5$ times the mount system frequency or $>= 35$ Hz. By comparison, the 3.2:1.0 ratio suggested by Racca [9] implies the mounted structure frequencies should be $>= 22.4$ Hz. Although the comparative study [11] did not examine the 3.2:1.0 ratio, a comparison between the 2:1 and 5:1 results suggests the 3.2:1.0 ratio would provide a good approximation to rigid body.

Steinberg [10] suggests an "Octave Rule" in which a frequency ratio greater than 2:1 be used to sharply reduce dynamic coupling. This will subsequently reduce the response of the structure. Figure 2 (taken from Steinberg [10]) depicts shock amplification versus frequency ratio, R, and illustrates application of the Octave rule. The two mass diagram in Fig. 2 shows a PCB mounted to a box that is isolated by mounts with critical (Cr) damping of 0.10 and a transmissibility, Q, of 5. The amplification for several values of PCB mount damping are plotted. The Octave rule suggests the use of isolators with frequencies that are $<= 1/2$ the frequencies of the above mount items. This is shown by the hashed region of Fig. 2 and keeps the system out of the dangerous amplification area. Worth noting is the fact that higher damping values reduce the amplification. However, higher damping tends to increase excitation levels across a larger bandwidth. This may in turn increase the response [14] of components during shock that would otherwise have a small response.

During shock qualification testing [12], sustained [7] frequencies from complex transients are likely to excite equipment modes above the mounts. They may originate from deck simulator fixtures tuned between 8 Hz to 30 Hz and transmit through (at a reduced level) to the equipment via the mounting system. In this case, the structure to forcing frequency ratio of 2:1, as discussed by Crede and Ruzicka [11], would require the minimum natural frequencies of the chassis and components (not the mount system) to be greater than 16–60 Hz respectively. These frequencies would sharply reduce responses. According to Steinberg [10], natural frequencies of electronic equipment on ships and submarines should be $>=$60 Hz. With increased use of COTS cabinets and components, the likelihood is that equipment with considerably lower natural frequencies are being introduced to the ship. One approach to deal with these cases is to use lower frequency mounting systems. However, the available mount stroke and excursion space may become limiting factors. Another approach is to stiffen low frequency components in system until they are at least one octave away from the expected forcing frequency of the qualification test. These components may be identified via exploratory vibration tests. In some cases, application of dynamic absorbers [15] may provide solutions. However, this may require application of more complex analytical methods.

To examine the case where rigid body theory may not be applicable, an analysis by Scavuzzo and Lam [13] was reviewed. In this study, normal mode theory was applied to investigate decoupling of a multi-mass vibration system. For this investigation, the first 10 seconds of an earthquake time history, having peak forcing frequencies between 8–10 Hz ($\sim$9 Hz), was applied to a primary single mass system having a natural frequency of 5 Hz. The response spectrum of the primary single mass system was then used a baseline to compare responses when a series of interacting masses having fixed base frequencies of 2.5 Hz, 5 Hz, and 7.5 Hz were added. This investigation concluded that for the cases studied, a single mass system (or rigid body) could not be used to estimate the effects of a multi-mass system. This corroborates the investigation presented by Crede and Ruzicka [11] where the structure to forcing frequency ratio must be at least 2:1 and the suggested structure to mount system natural frequency ratio must be at least 3.2:1.0. For example, the ratio of the fixed base frequencies of the added masses to peak earthquake forcing frequencies result in values of 2.5/9, 5/9, and 7.5/9 respectively. All of these are significantly less than the 2/1 ratio necessary for applying rigid body theory. The corresponding structure to mount system

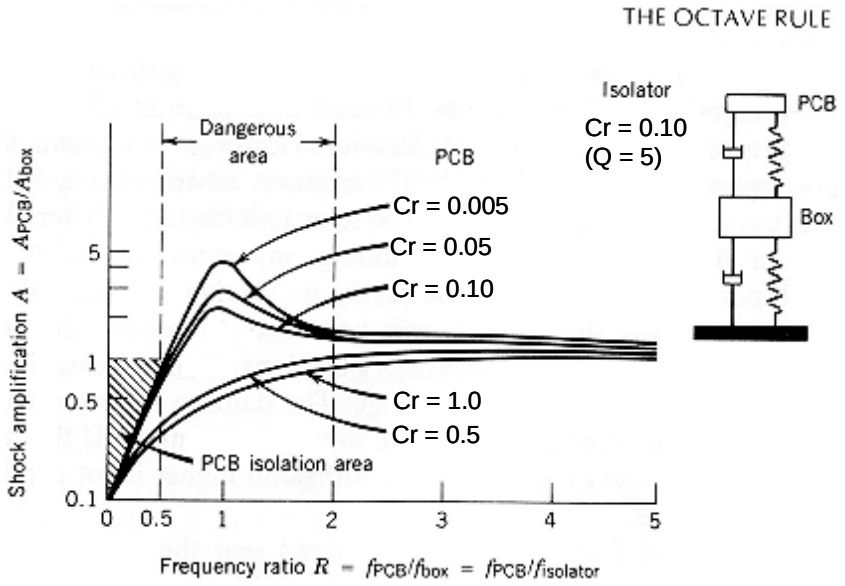

Fig. 2. Octave rule illustrated for 2 mass system.

natural frequency ratios in this study are 2.5/5, 5/5, and 7.5/5 respectively. Again, these are all considerable lower then the suggested 3.2/1.0 ratio.

2.2. Defeciencies of other methods

Existing [1,7,10,11,14–18] engineering methods have some or all of the following deficiencies: 1) no consideration for rotational effects; 2) lack of ability to easily change parameters; 3) lack of ability to account for variances; 4) they require considerable knowledge to use; 5) they overcomplicate the modeling assumptions necessary to obtain acceptable estimates of acceleration levels & displacements, and 6) they are difficult to calibrate.

According to Crede [11], "it is necessary to consider freedom of movement in all directions, as dictated by existing forces and motions and by the elastic constraints. Thus in the general problem, the equipment is considered a rigid body supported by resilient supporting elements or isolators." Calculation of accelerations and displacements without accounting for simultaneous rotations or coupled [18] rigid body modes can lead to erroneous and sometimes detrimental results. For example, rotation of a mounted system may generate responses that exceed an allowed excursion space possibly impacting nearby equipment, structures, or even people. Fragility [17] levels may be exceeded during rotation and are very likely to be exceeded during an impact. Hand calculations; shock response spectra; mount sizing nomographs, tables, & charts; and other mount application tools [14,17] that leave out rotational effects will be inadequate for estimating excursions in 3 dimensional (3D) space.

The best way to estimate and insure that fragility levels and excursion constraints are not exceeded is to calculate the acceleration levels and displacements from a 3D or 6DOF model where rotational effects can be estimated.

Many investigations have been performed to characterize isolators with the least amount of variance possible. Care must be taken to distinguish between characterizations for shock applications and those for vibration isolation. For example, the vibration [3,9] characterization of several kinds of rubber mounts has revealed that for small vibration displacements, the dynamic-to-static stiffness ratio increases when the rubber durometer increases. Richards and Singh [3] suggests that mount shape plays a role in determining this ratio. For example, they [3] reported a dynamic stiffening of 2 to 2.5 times the static stiffness for a "neoprene (30 durometer) bubble-type isolator with a hollow cavity" having a non-linear load deflection curve and damping between 6.9 and 7.6% Cr. This was based on vibration tests where the root mean square force was on the order of one Newton. At this force level, the resulting displacements, based on the static load test data [3, p. 815] of that mount, is about 1 millimeter. The resulting stiffness in that region (in the direction of loading) is about 2.2 times stiffer than the model used

in that study. If the actual stiffness of the mount were used in lieu of the model stiffness, the ratio of dynamic to static stiffness would most likely be about 1 to 1.1 which is similar to other mounts cited in the study and would agree with results presented by Racca [9]. However, this effect may not be as significant when large deformations [4] occur in the mounts. For shock applications, Hain and others [17] suggest the static stiffness for natural rubber is approximately equal to the dynamic stiffness, but for medium and highly damped elastomers, this ratio would be 1.3 and 1.5 respectively.

Many wire rope and non-rubber elastomeric shock mounts with all types of shapes and loading curves are used in industry. It would be impractical to dynamically characterize each of them for shock applications. A more practical approach is to use available information from vendors and handbooks [9] to estimate their variances and calculate the effect on the equipment response. If the equipment response is acceptable over the range of the variance, dynamic characterization may not be needed. However, existing 3D models used for shock simulation are not efficient when it comes to making changes or accounting for variances in model parameters such as component weight & dimensions, mass moments of inertia, mount locations, mount orientations, mount load-deflection characteristics and damping, cabinet or component orientation to shock, input & output data, and others.

Accounting for variances requires some knowledge of the uncertainties and range of validity associated with the parameters being estimated. Implementing and assessing the impact of the variances will require multiple calculations from calibrated models using 6DOF analysis tools. This may be done manually one simulation at a time or automatically with Monte-Carlo simulations [15,19,20] to perform multivariate and univariate sensitivity analyses. Most 6DOF analysis tools such as finite element codes and specialized simulation tools require an [14,16] extensive working knowledge and expertise to build and simulate models for shock isolated systems. Calibrating and implementing multivariate and univarite sensitivity analyses with such tools would be even more complicated and time consuming.

The SIMPLE simulation method developed for this study addresses question 2 by providing comprehensive solutions to the above issues in a practical and efficient manner. It provides a template for modeling the isolated systems as 6DOF rigid bodies. The template can be changed as necessary to assess, confirm, iterate, and compare designs (e.g. trade studies). This includes selection of mounts from a library to save time when specifying mount properties. In addition, variances can easily be assigned to model parameters and sensitivity analyses run. Calibration of model parameters with measured data can also be performed. No special knowledge is required to use SIMPLE and no overcomplicated modeling assumptions are necessary to obtain reasonable estimates of isolated system responses.

3. Theory base for simple simulation method

SIMPLE integrates concepts and theories from other fields such as rigid body dynamics, shock and vibration theory, rotational matrices, elastic beam theory, systems dynamics, and multivariate sensitivity analysis. Each concept or theory and how they are implemented are discussed briefly.

3.1. Rigid body dynamics theory

SIMPLE incorporates motion of a rigid body in three dimensions. Figure 3 shows a cabinet (or rigid body) where the component forces F_x, F_y, F_z of $\vec{F}$ at each mount; components of angular velocity Ω; and angular momentum $\vec{H}_G$ are defined with respect to the rotating reference frame $GX'Y'Z'$. In this system, $\vec{r'}$ represents the locations of mount force application points on the rigid body with respect to the mass center "G". The goal here is to determine relative displacements $\vec{\delta}$ and accelerations $\ddot{\vec{r'}}$ at the mounts and other points on the rigid body. To do this, the basic equations of motion [21] are simultaneously solved and integrated to find the velocities $\dot{\vec{r'}}$ at each point on the rigid body. Subtracting these velocities from the input velocities provides the relative velocities that are then integrated to obtain $\vec{\delta}$. To obtain acceleration $\ddot{\vec{r'}}$ for each point, the velocities $\dot{\vec{r'}}$are simply differentiated. The basic equations of motion employed in SIMPLE are:

$$\sum \vec{F} = m\ddot{\vec{r'}}_G \tag{1}$$

$$\sum \vec{M}_G = (\dot{\vec{H}}_G)_{GX'Y'Z'} + \Omega \times \vec{H}_G \tag{2}$$

where m is the rigid body mass, $\ddot{\vec{r'}}_G$ is the acceleration at the mass center "G", $\vec{M}_G$ are the moments about "G" of applied forces; and $(\dot{\vec{H}}_G)_{GX'Y'Z'}$ is the rate of change of angular momentum $\vec{H}_G$ with respect to the rotating frame $GX'Y'Z'$. The relation $(\dot{\vec{H}}_G)_{GX'Y'Z'}$

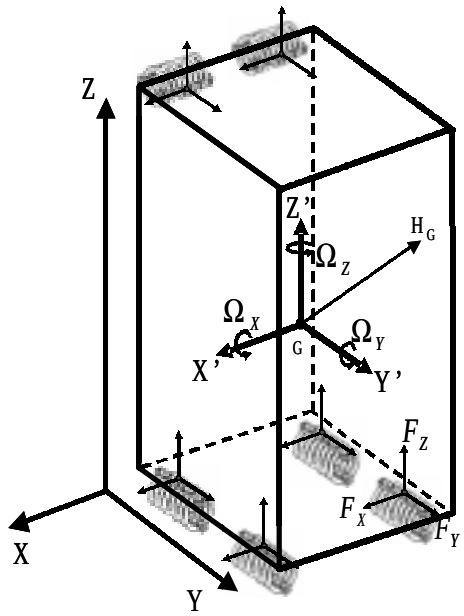

Fig. 3. Rigid body approximation of cabinet.

is determined by:

$$(\dot{\vec{H}}_G)_{GX'Y'Z'} = \frac{d}{dt}\vec{H}_G = \frac{d}{dt}\begin{vmatrix} Ix & -Pxy & -Pxz \\ -Pyx & Iy & -Pyz \\ -Pzx & -Pzy & Iz \end{vmatrix} \begin{bmatrix} \Omega_x \\ \Omega_y \\ \Omega_z \end{bmatrix} \quad (3)$$

where the matrix of Eq. (3) represents the inertia tensor of the cabinet at its mass center "G." Expressions for $\vec{M}_G$ are found from the following relation:

$$\vec{M}_G = \vec{r''} \times \vec{F} \quad (4)$$

where the vector $\vec{r''}$represents the distance from the mass center "G" to the elastic center [18] of the shock mount (e.g. $\vec{r'}$ plus the approximate height of the mount for wire rope mounts). SIMPLE simultaneously solves Eqs (1)–(4) to determine the translational accelerations $\dot{\vec{r'}}$ and angular velocities Ω at the mass center "G" of the rigid body. These are then used to determine velocity $\dot{\vec{r'}}$ at each point from the following relation:

$$\dot{\vec{r'}} = \int \ddot{\vec{r'}}_G dt + \Omega \times \vec{r'} \quad (5)$$

3.2. Shock and vibration theory

SIMPLE calculates both un-damped and damped forces for each mount location. The un-damped forces are calculated in SIMPLE for the X', Y', and Z' directions using mount force-deflection lookup tables often referred to as load-deflection (L-D) curves. The damped forces are determined from coefficients or estimates of critical damping. The input of a mount lookup table is relative displacement $\vec{\delta}$ and the output is force. Relative displacement $\vec{\delta}$ is calculated in SIMPLE using the following relation:

$$\vec{\delta} = \int (\dot{\vec{r''}} - \dot{\vec{r'}})dt \quad (6)$$

where $(\dot{\vec{r''}} - \dot{\vec{r'}})$ is the relative velocity between the elastic center of the shock mount and the point where the mount connects to the rigid body. Damping forces $\vec{F}_{\hat{r}i_{\text{damping}}}$ for the ith mount are calculated from the following relation:

$$\vec{F}_{\hat{r}i_{\text{damping}}} = c_{\hat{r}_i}(\dot{\vec{r''}}_i - \dot{\vec{r'}}_i) = 2\zeta_{\hat{r}_i}K_{\hat{r}_i}\sqrt{\frac{m}{\sum_i K_{\hat{r}_i}}}(\dot{\vec{r''}}_i - \dot{\vec{r}}'_i) \quad (7)$$

where $c_{\hat{r}_i}$ is the damping coefficient, $\zeta_{\hat{r}_i}$ is the percent critical damping, and $K_{\hat{r}_i}$ is the stiffness (e.g. slope of L-D curve) of the ith mount in the $\hat{r}$ direction.

In SIMPLE, L-D curves are specified for the principal elastic axes of compression-tension (CT), shear, and roll. Sometimes mount vendors will designate a principal axis to be at a 45 degree angle depending on the application of the mount. Torsional stiffness is typically neglected [18] when the size of the rigid body is large compared to the mount. When rigid body dimensions are small compared to the mounts (e.g. less than 2:1), SIMPLE allows torsional stiffness to be approximated by distributing the mount load to more than one elastic center. Figure 4 shows the orientation of the principal elastic axes on a wire rope mount. The numbers assigned to each principal axis corresponds to the nomenclature SIMPLE uses to identify mount direction forces with the appropriate L-D lookup. Mounts may also be rotated at any angle with respect to the rigid body coordinate system.

Figure 5 shows an example of damped and undamped L-D responses calculated in SIMPLE for the CT cycles of a mount. Although L-D hysteresis loops may be employed [1,4,5] to approximate damping, the SIMPLE template is set up to use values for either $c_{\hat{r}_i}$ or $\xi_{\hat{r}_i}$ to calculate damping forces in accordance with Eq. 7.

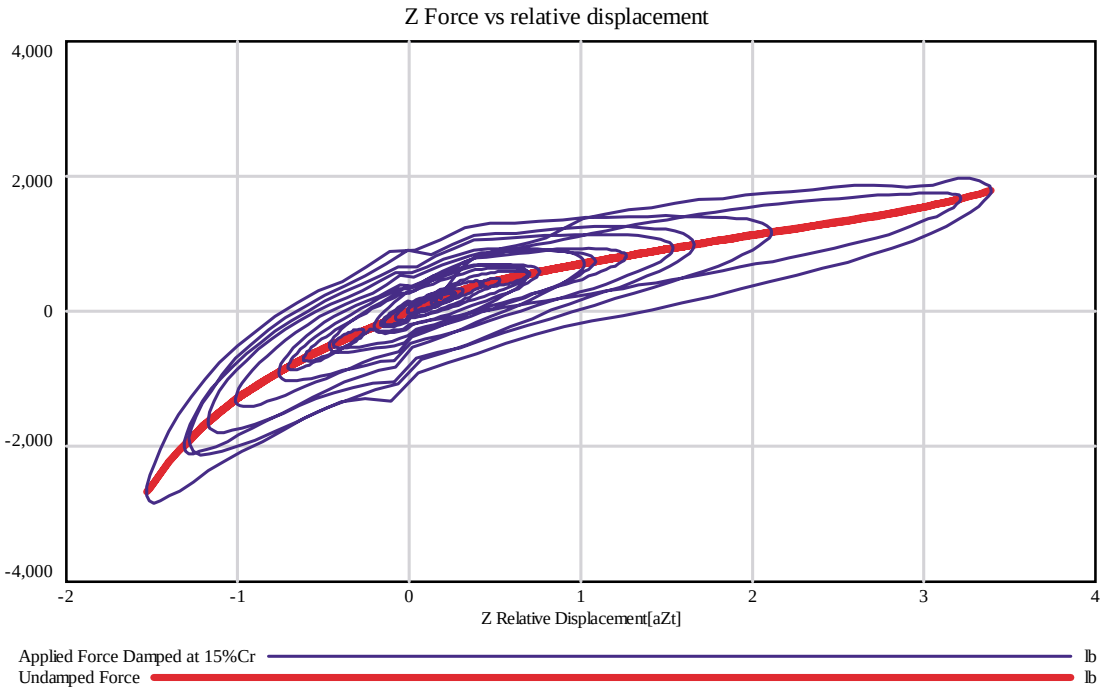

Fig. 5. Example of L-D response.

$$|\vec{V}'\rangle = \mathbf{A}|\vec{V}\rangle = \begin{vmatrix} \cos\theta_y \cos\theta_z & \cos\theta_y \sin\theta_z & -\sin\theta_y \\ (\sin\theta_x \sin\theta_y \cos\theta_z - \cos\theta_x \sin\theta_z) & (\sin\theta_x \sin\theta_y \sin\theta_z + \cos\theta_x \cos\theta_z) & \sin\theta_x \cos\theta_y \\ (\cos\theta_x \sin\theta_y \cos\theta_z + \sin\theta_x \sin\theta_z) & (\cos\theta_x \sin\theta_y \sin\theta_z - \sin\theta_x \cos\theta_z) & \cos\theta_x \cos\theta_y \end{vmatrix} \begin{bmatrix} V_x \\ V_y \\ V_z \end{bmatrix} \quad (8)$$

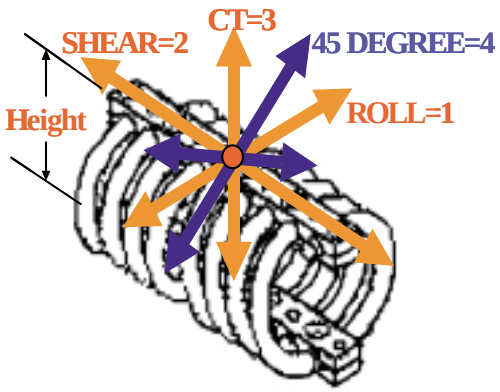

Fig. 4. Principal elastic axes.

3.3. Rotational matrices

SIMPLE allows the rigid body to be rotated at any angle with respect to the input reference frame as shown in Fig. 6. For example, this may happen when complying with MIL-S-901D test requirements [12], where a cabinet may be rotated an angle of $\theta_z = 90$ degrees about the Z axis on a heavy weight test and inclined by an angle of θ_x or $\theta_y = 30$ degrees on a medium weight test. Rotation directions for angles θ_x, θ_y, and θ_z are positive in the counterclockwise direction. SIMPLE uses the rotation matrix $\mathbf{A}$ as shown in Eq. 8 and its inverse $\mathbf{A}^{-1}$ when transforming in and out of the rigid body frame and reference frame. Matrix $\mathbf{A}$ was derived from multiplying matrices of successive [22] rotation. With this matrix, input velocities $\vec{V}$ of the input reference frame are transformed into input velocity $\vec{V}'$ of the rigid body frame. In order to calculate the reference input velocities $\vec{V}$, the coordinates $\vec{r}$ with respect to the input reference frame must be determined.

SIMPLE does this by transforming the locations of the mount elastic centers $\vec{r}''$ from the rigid body frame over to the input reference frame and then adds the reference frame distance $\vec{r}_G$ of the mass center "G" using the following expression $|\vec{r}\rangle = \mathbf{A}^{-1}|\vec{r}''\rangle + \vec{r}_G$. This is important when the reference frame is rotating, since there will be a significant change in the input velocities the farther $\vec{r}$ is from the origin. For example, velocities at sway mounts located high on a cabinet will be higher than velocities at the base mounts when being

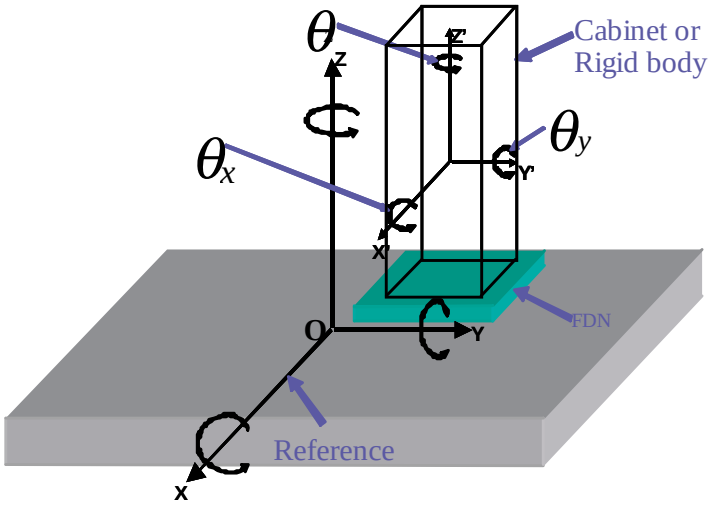

Fig. 6. Rigid body orientation to input reference frame.

tested on floating shock platforms and deck simulators where rotations occur.

The same rotation matrix and its inverse are used for rotating the mounts at their point of attachment to the rigid body. This allows mounts principle elastic axes to be positioned at any angle before simulating. Isolated systems undergo small dynamic rotations of +or-10 degrees with respect to the input reference frame when subjected to shock. Based on this, no dynamic rotational transformations are made in SIMPLE between the elastic centers of the mounts and the points where they attach to the cabinet when calculating relative velocities $(\dot{\vec{r}}'' - \dot{\vec{r}}')$.

3.4. Application of elastic beam theory

Inputs used in SIMPLE can be arbitrary 6 degrees of freedom or selected from a variety of inputs based on models and test data. Both translation and rotation terms for input $\vec{V}$ are combined in an expression similar to Eq. 5. Analyses of isolated system performance on deck simulator fixtures (DSFs) and floating shock platforms (FSPs) used in MIL-S-901D heavy weight testing are frequently requested. A typical heavy weight test configuration is shown in Fig. 7 where the direction of the shock input with respect to the reference frame is depicted. Locations of cabinets on a DSF are also depicted in this figure. SIMPLE is defaulted to select inputs based on a 20' horizontal charge standoff. However, other standoffs between 20' and 30' can be selected.

When DSF or FSP test data inputs are selected, SIMPLE automatically augments the data (e.g. recorded vertical and athwartship time histories) with rotations. DSF inputs, when selected, incorporate deck deformations along the Y directions in the reference frame as shown in Fig. 8 where Δ is the max response at the centerline of the DSF corresponding to $Y_{\text{ref}} = 0$. This causes the inputs to vary depending on where the equipment is located. An expression for the DSF deformation along Y is estimated by normalizing and superimposing [23] equations for the elastic curve of a beam subject to uniform loading "**wL**" and point loads "**P**" symmetrically placed at "**a**" as shown in Fig. 8. Equation 9 below [24] represents the normalized elastic curve implemented in SIMPLE where γ is the % contribution associated with the shape generated by the point loads. The value of γ and the placement "**a**" of the point loads can be changed in SIMPLE to better represent the configuration of loading on the DSF.

$$\begin{aligned}\text{Elastic curve} = (1-\gamma)\left(\frac{16}{5L^4}\right)\Bigg\{&\left(Y_{\text{ref}} - \frac{L}{2}\right)^4 \\ &-2L\left(Y_{\text{ref}} - \frac{L}{2}\right)^3 \\ &+L^3\left(Y_{\text{ref}} - \frac{L}{2}\right)\Bigg\} \\ &+\gamma\left(\frac{4}{(3L^2-4a^2)}\right)\end{aligned} \tag{9}$$

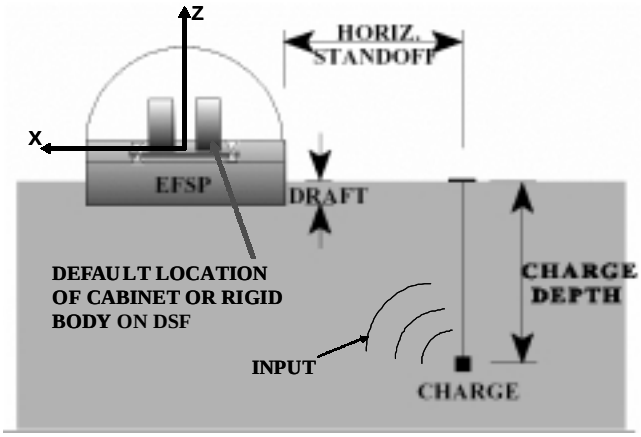

Fig. 7. Typical heavy weight test configuration.

$$\begin{cases} \left\{3L\left(Y_{\text{ref}}-\frac{L}{2}\right)-3\left(Y_{\text{ref}}\right.\right. \\ \left.\left.-\frac{L}{2}\right)^2-a^2\right\} \\ \text{for } \left(Y_{\text{ref}}-\frac{L}{2}\right)\geqslant a \text{ and } \left(Y_{\text{ref}}\right. \\ \left.-\frac{L}{2}\right)\leqslant (L-a) \\ \left(Y_{\text{ref}}-\frac{L}{2}\right)\left(\frac{1}{a}\right)\left\{3La-3a^2\right. \\ \left.-\left(Y_{\text{ref}}-\frac{L}{2}\right)^2\right\} \\ \text{for } \left(Y_{\text{Ref}}-\frac{L}{2}\right)<a \text{ and} \\ \left(Y_{\text{ref}}-\frac{L}{2}\right)>(L-a) \end{cases}$$

SIMPLE implements Eq. 9 as an interpolation factor between the DSF velocities V_{zDSF} at $Y_{\text{ref}}=0$ and the FSP velocities V_{zFSP} at the pinned locations where $Y_{\text{ref}}=+\text{or}-L/2$. This is shown below in Eq. 10.

$$V_z=(V_{zDSF}-V_{zFSP})\text{Elastic curve} +V_{zFSP} \tag{10}$$

SIMPLE also uses Eqs 9 and 10 to calculate the rotational inputs induced by DSF deformation at the foundations below the isolated systems. These rotations increase the Y direction DSF velocities $V_{Y\ DSF}$ for points above the cabinet foundations (e.g. sway mount locations) as you move the foundations farther from the athwartship centerline of the DSF at $Y_{\text{ref}}=0$.

3.5. Systems dynamics programming

SIMPLE uses systems dynamics programming to integrate causal relations into feedback loops so that system behaviors such as growth, decay, oscillations, etc. can be examined. Shock isolated systems are characterized as 2nd order feedback loops in the SIMPLE program. A systems dynamics simulation environment called Vensim by Ventana Systems, Inc provides the workbench for programming the causal relations as well as the simulation and outputs necessary to examine behavior.

Using SIMPLE to build your own model from a template allows users to quickly and easily build and simulate models customized to their needs. During simulation setup in SIMPLE, general parameters such as rigid body weight, dimensions, mass moments of inertia, mount locations, mount orientations, mount characteristics, cabinet orientation to shock, input data, and others can be varied using a graphical interface. Load deflection (L-D) curves characterizing shock mounts may be entered into lookup tables manually, imported from other applications, or selected from mount libraries. Elastic axes of the L-D curves, such as compression-tension, shear, and roll can be selected and orientated for up to 22 mount locations. Damping and mount scale factors are also implemented for each mount in each direction. This provides ability to account for variances such as dynamic stiffening. In the Vensim environment [20], three types of integration techniques are available: Runge Kutta, Euler, and Difference. SIMPLE is set to use the Runge Kutta 2nd order fixed time step integration method for simulations.

3.6. Multivariate sensitivity analysis

The Vensim simulation environment provides SIMPLE with a graphical interface to setup and run multivariate sensitivity simulations using the Monte Carlo simulation technique. Hundreds or even thousands of simulations can be performed while randomly sampling the parameters over a range of values. The number of simulations, parameters to vary and the type of distribution for the variance are all selected from a graphical

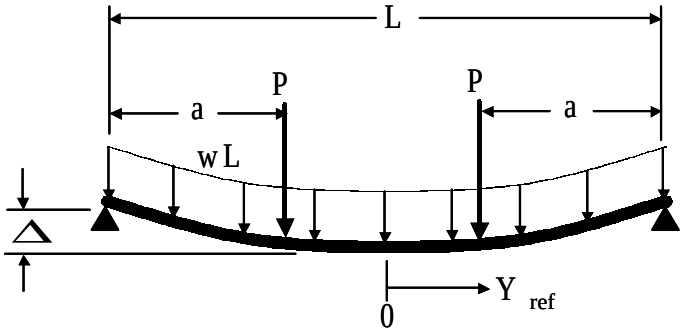

Fig. 8. Beam diagram for DSF.

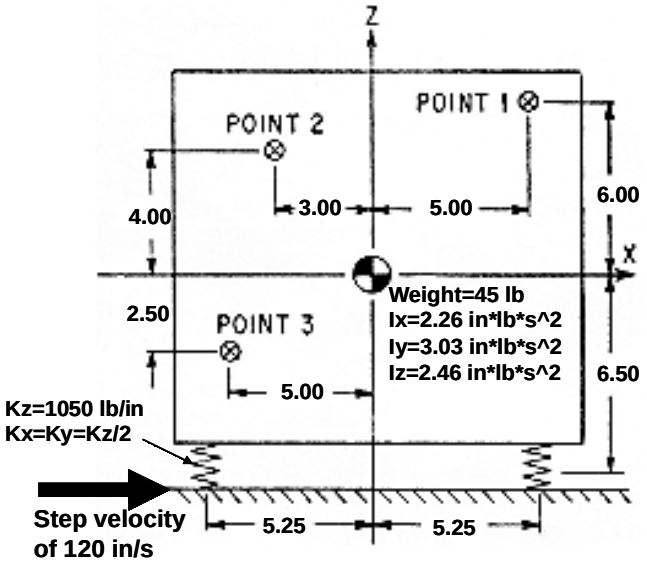

Fig. 9. 2 planes of symmetry.

interface dialog box. Up to 12 types of distributions such as Uniform, Normal, Poisson, Binomial, Beta, Exponential, Gamma, etc. are selectable for defining parameter variance.

4. Validation of simple predictions by benchmarking

To answer question 4, two rigid body sample problems are used to benchmark the SIMPLE simulation method. They are taken from Himelblau and Sheldon's [18] chapter on "Vibration of a Resiliently Supported Rigid Body," found in the Shock and Vibration Handbook, 3rd Ed. by Harris. The first problem addresses a rigid body having two planes of symmetry with a translational shock to its foundation. The objective with this problem is to validate SIMPLE's capability to predict the coupled modes of a rigid body and effects from damping. The second problem addresses a rigid body with one plane of symmetry having rotational velocity shock. The objective is to use the rotational shock, which generates input along two axes, to validate or corroborate SIMPLE's capability to predict responses from a coupled mode system having multiple inputs.

4.1. Two planes of symmetry with translational velocity shock

For this benchmark, responses of a rigid body with two planes of symmetry are compared at three points. They are labeled points 1, 2, and 3 as shown in Fig. 9 (taken from Himelblau [Reference 18, page 3–19]).

Table 1
Peak response comparisons

Response	Himelblau	SIMPLE	% Diff
Y acceleration at CG	0.74 g's	0.72 g's	2.8%
Z acceleration at CG	4.09 g's	4.11 g's	0.5%
Angular Acceleration about X Axis	45.9 rad/s^2	46.2 rad/s^2	0.7%

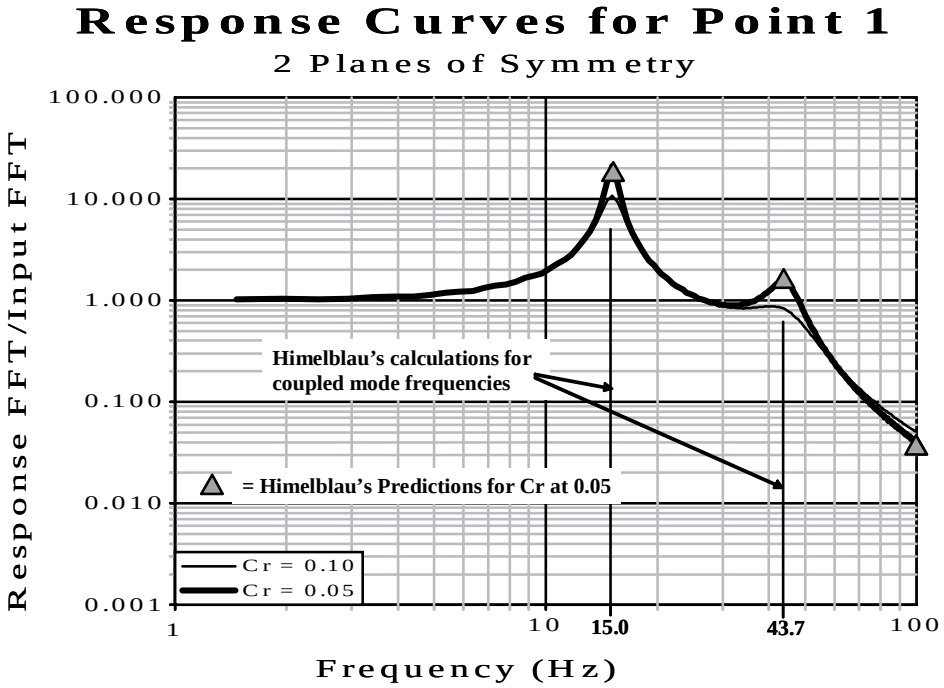

Fig. 10. Response curves for point 1.

The planes of symmetry are the XZ and XY planes and the input is a 120 in/s velocity step in the X direction at the foundation. Parameter values such as the weight, inertias, mount locations, and stiffness as shown in the figure were used in SIMPLE to calculate responses for the 3 points. These correspond to the same values used by Himelblau [18] to calculate responses from a digital computer for several different values of damping.

Results from SIMPLE are shown in Figs 10, 11, and 12 which depict the transmissibility plots for the 3 points. Transmissibility plots were obtained by taking the ratios of the Fourier transforms of the responses and input in the X direction. The calculated uncoupled mode natural frequencies are 21.4 Hz in the X direction, 30 Hz in the Z direction, and 41.4 Hz about the Y axis. Values for the coupled mode frequencies of 15 Hz and 43.7 Hz, as calculated by Himelblau, are depicted on the abscissa and correspond to the modes calculated by SIMPLE. Each figure also compares the responses for mount damping values set to Cr $= 0.05$ and 0.10. Maximum and minimum values presented by Himelblau [18] for the Cr $= 0.05$ case are plotted in the figures for comparison. These results confirm the capability of SIMPLE to accurately predict rigid body coupled modes and responses where damping is present.

Acceleration and relative displacement time histories for Point 1 are compared to those at the top of the mounts as shown in Figs 13 and 14 respectively. The accelerations (Fig. 13) at these two locations are initially out of phase and are responding in a different mode. They eventually take on the same phase and mode, but at different amplitudes. The relative displacements in the X direction (Fig. 14) show a difference of $\sim$1.1 in. between the mounts, which are at the base, and Point 1, near the top. An SRS analysis would not reveal this difference. This confirms the need for performing a 6DOF analysis where coupled modes are simulated.

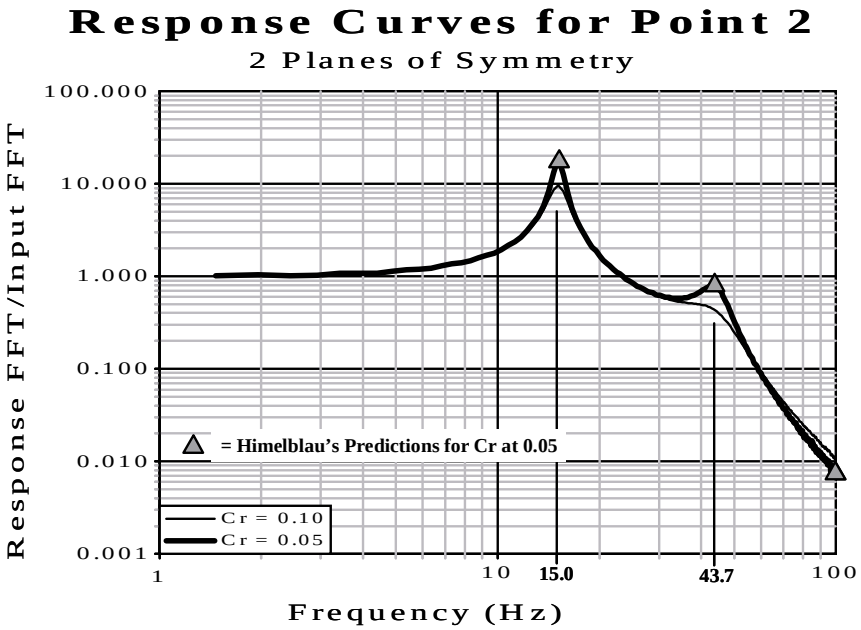

Fig. 11. Response curves for point 2.

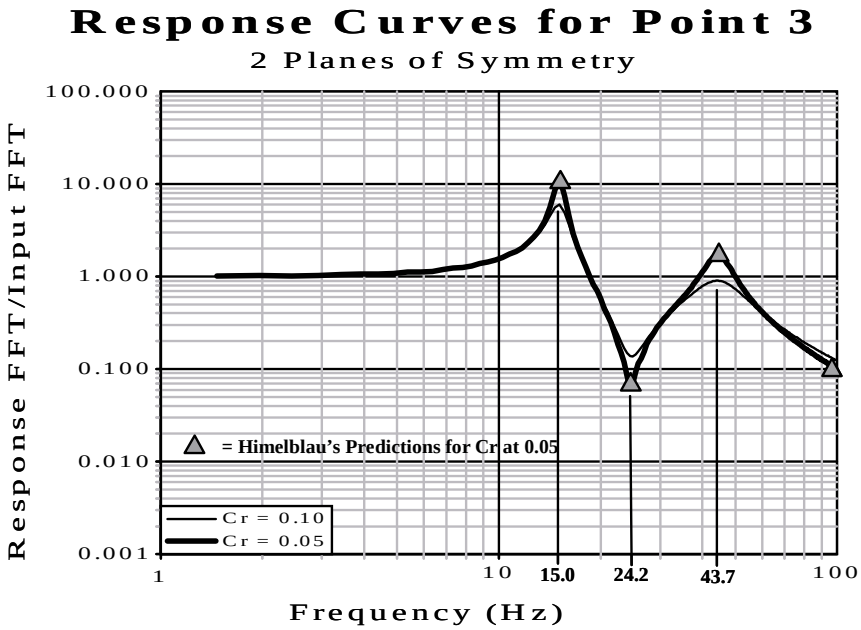

Fig. 12. Response curves for point 3.

4.2. One plane of symmetry with rotational velocity shock

A second benchmark comparison with Himelblau's rigid body calculations was made with a system having one plane of symmetry as shown in Fig. 15. The system was subjected to a rotational shock velocity of 0.38 rad/s; a result of a drop where one end was raised to a height of 36 inches. The overall weight, inertia, dimensions, and locations of mounts are shown in the figure. For this system, mounts apply forces only along the longitudinal axes. The calculated natural fre-

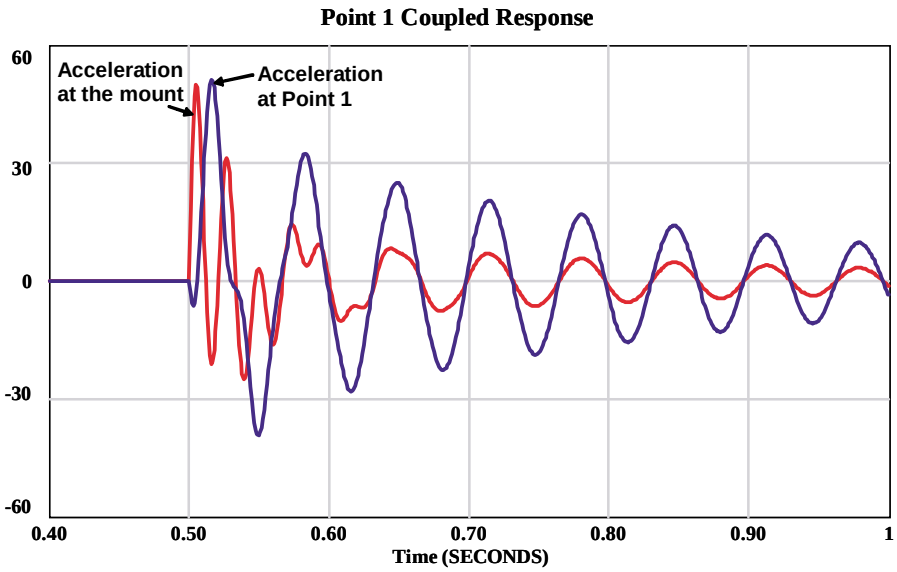

Fig. 13. Acceleration comparison between point 1 and just above the mount.

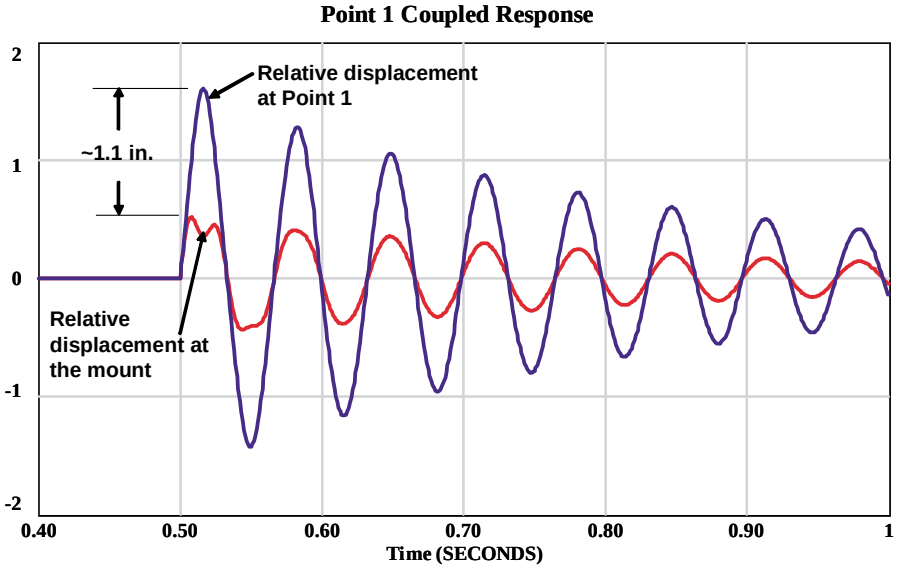

Fig. 14. Relative displacement comparison between point 1 and just above the mount.

quency in the Z direction is 7.22 Hz and the coupled frequencies, as calculated by Himelblau, are 3.58 Hz, 6.02 Hz, and 9.75 Hz. These values agree with SIMPLE simulations as shown in Figure 16. In this figure, the response of the system at the center of gravity is plotted as a function of frequency for the Y and Z directions. Comparisons between SIMPLE and Himelblau's calculations for peak responses at the center of gravity (CG) are shown in Table 1 for the case where Cr $= 0$. Differences are less than 1% for the angular and Z direction accelerations which corroborates the SIMPLE simulation method for rotational shock. Figures 17 and 18 show the predicted time histories for the Z and Y directions respectively. Each also depict the responses for Cr $= 0.1$ to illustrate the differences that occur in peak responses and phasing if damping is ignored. For example, in the Z direction (Fig. 17), the peak un-damped response is $\sim$1.2 times greater than the 10% damped response and occurs at a much later time. A similar scenario holds for the Y direction. The

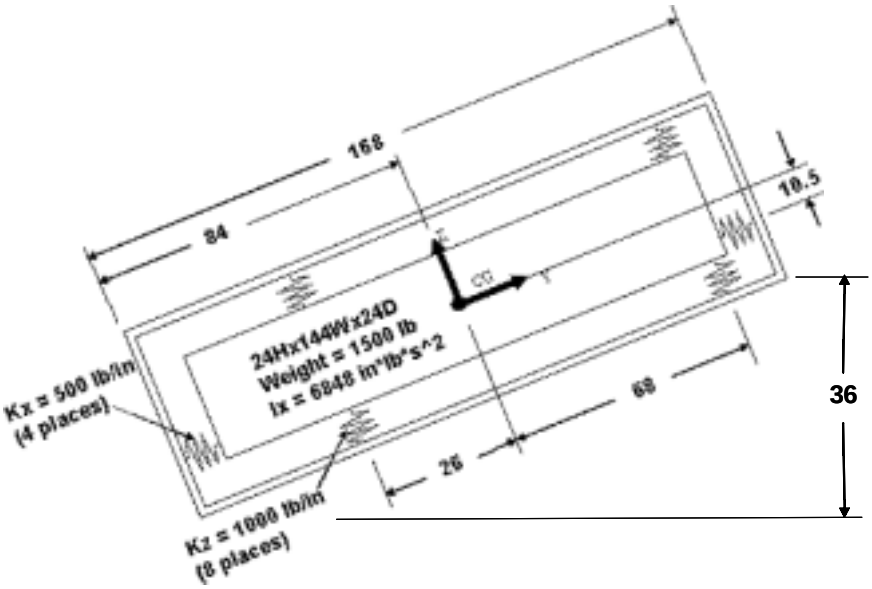

Fig. 15. System with one plane of symmetry.

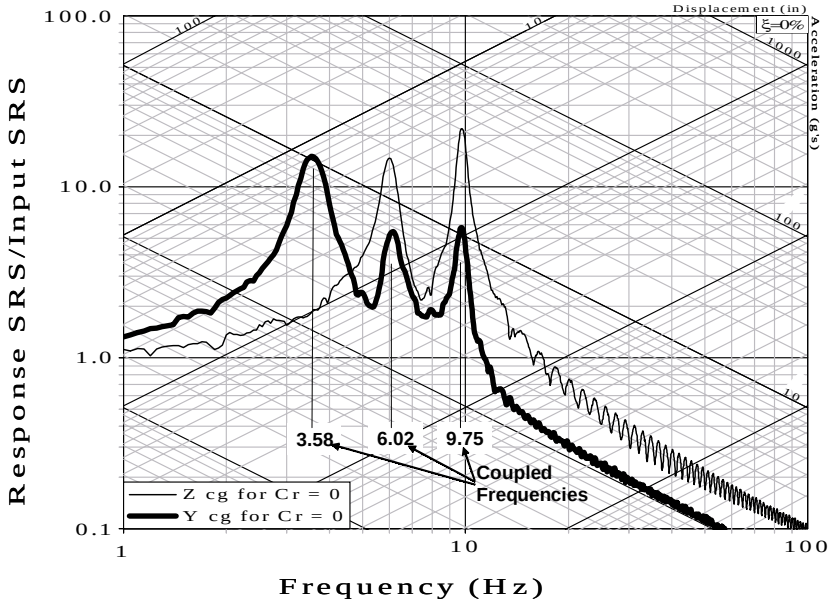

Fig. 16. Responses from SIMPLE simulation showing coupled frequencies.

differences would be greater at points farther from the center of gravity.

5. Application of process

Twenty-five of the 90 cabinets associated with the Smartship Integrated Ship Controls were classified as isolated equipment subject to MIL-S-901D [12] Type 2 heavyweight testing on 14 Hz & 30 Hz deck simulator fixtures (DSFs). Of the 25 cabinets, 15 were designated for actual testing with the remaining to be qualified by extension. It was necessary to identify mounts for these cabinets that would meet dynamic performance goals. It was also required that they interface well with the existing shipboard arrangements as well as the individ-

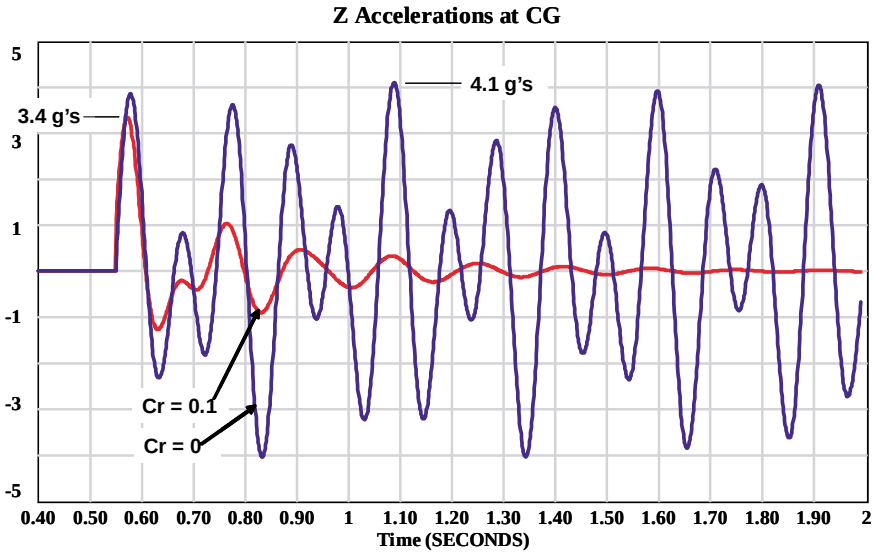

Fig. 17. Predicted time histories for Z acceleration at the center of gravity.

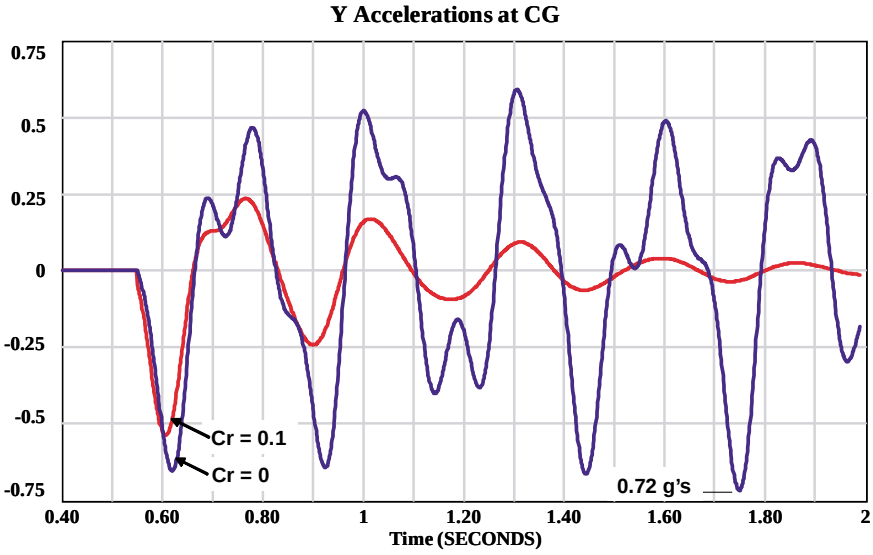

Fig. 18. Predicted time histories for Y acceleration at the center of gravity.

ual cabinet structures. The mount performance goals were to achieve cabinet acceleration levels around 15 to 25g's with excursion envelopes less than 4 inches. With the exception of one cabinet, these performance goals were met during shock tests conducted [26–28] from December 2001 to May 2002 at HI-TEST LABORATORIES, INC. in Arvonia, Virginia. Achieving the acceleration requirement during shock testing was a challenge since restraints on cabinet components such as batteries, power supplies, internal chassis, and cabinet doors were inadequate. Modifications were made to some of the cabinets to keep these items secure during testing. Meeting these performance goals contributed significantly to shock protection of these cabinets, all of which were successfully shock qualified and installed aboard ship thus validating the mount selection process described in this paper.

5.1. Application to assess

For two of the CG 47 Class Smartships, 14 cabinets were already installed on wire rope mounts that

were suspected of not having enough stroke available to accommodate the high relative displacements expected during testing on the DSF. The lack of sufficient stroke would cause bottoming and topping out of the mounts during tests. This would result in high "g" levels that may damage the structures and equipments isolated by the mounts. In some cases, the mounts might break, launching the equipment. This was evidenced during the shock testing [29] of Z-frame, C-frame, and A&J Rack configurations with similar wire rope mounts in support of the Navy's Integrated Condition Assessment System. A preliminary assessment of the already installed mounting systems was done to estimate the needed stroke and to compare it with the available stroke. This was accomplished using two methods: assessment using shock response spectra and simulations using SIMPLE.

5.1.1. Assessment of already installed cabinets using shock response spectra (SRS)

First, the approximate vertical natural frequencies for each of the isolated systems were calculated. Next, the vertical SRS of DSF test data was calculated so that the dynamic relative displacements at the previously calculated natural frequencies could be read from the graph. To come up with a number for the needed stroke in the mount, estimates of additional displacements associated cabinet rotations and equilibrium offsets were added to the dynamic relative displacements read from the SRS. Comparisons of available stroke in the mounts to the needed stroke for testing (based on SRS) were then made.

The vertical natural frequencies of the isolated systems ranged from 6.6 Hz–8.7 Hz with 70% of them having a natural frequency between 7 Hz–7.5 Hz. These frequencies are calculated using $\sqrt{(g/w)\sum k}$ where g is acceleration of gravity (e.g. 386.4 in/s^2), W is the weight of the system, and $\sum K$ is the sum of stiffness values of all the mounts in the vertical direction. Since wire rope mounts are nonlinear, a single value of K for each mount force-displacement curve must be determined. This is accomplished using the relation between work and potential energy. For example, solving for K in the expression $\int F d\delta = K\delta^2/2$ using the trapezoidal rule [30] to evaluate the integral leads to

$$K = \frac{2}{\delta_N^2}\sum_{i=1}^{N}\{(\delta_i - \delta_{i-1}) * [F(\delta_{i-1}) + F(\delta_i)]/2\} \tag{11}$$

where δ_N is the largest expected relative displacement on the force displacement curve corresponding to point N and the summation from i = 1 to N is the area under the force displacement curve corresponding to the work.

The SRS of 13 Hz DSF data with 10% Cr, as shown in Fig. 19, was used for the assessment. A damping value of 10% Cr was selected over that of the nominal 15% Cr [9] for wire ropes in order to get a more conservative estimate of the relative displacement. This figure shows that for a 7 Hz linear system, 3 inches of dynamic displacement would be needed to achieve a 15g response. Displacements at all other frequencies less than the DSF frequency (e.g. 13 Hz) would be higher than 3 inches.

Table 2 summarizes the evaluated isolation systems and includes the unit name and drawing number, mount part numbers, unit weight, approximate natural frequencies, available mount stroke, and needed mount stroke. Equilibrium and rotational offsets were estimated to be between 0.2 to 0.3 inches and are included in the column for needed stroke. Comparison of the available and needed stroke columns show that all of the mounts will likely bottom during shock testing with the DSF tuned to 13 Hz.

This analysis was also performed using an SRS plot from 14 Hz DSF data with damping at 15% Cr as shown in Fig. 20. In the bandwidth from 6–8 Hz, the dynamic relative displacement ranges from 2.6–3.0 inches. With the higher frequency deck and damping, the available mount stroke is still inadequate even without considering the equilibrium and rotational offsets. Figure 20 also presents the SRS of 8 Hz DSF data depicting even higher dynamic relative displacement for the 6–8 Hz bandwidth. It can be generalized from the SRS analysis that the existing mounting systems will bottom on any DSF tuned between 8–16 Hz.

Based on results of the SRS and the allowance for equilibrium offsets and rotations, it was determined that the mounting systems should have an available stroke $>=$ 3.6 inches in compression for vertical natural frequencies in the range of 6–8 Hz. According to Hain and others [17], a good rule to follow to prevent bottoming is to allow a clearance space equal to 1.4 times the maximum dynamic relative displacement. For example, the clearance space needed for a mount system having a 2.6 to 3 inch dynamic displacement is $\sim$3.7 to 4.2 inches. Application of the Hain rule and the approach of adding allowances appear to give similar results in this case. This rule may not be valid for systems where significant sway may occur or when uncertainties in the inertial and mount properties are high. In those cases, additional sensitivity analysis may be necessary.

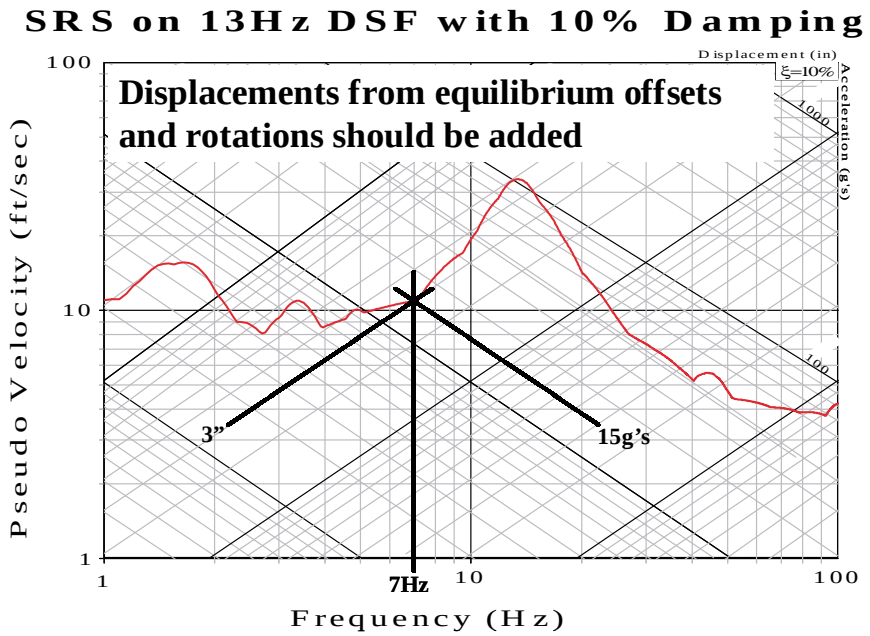

Fig. 19. SRS of 13 Hz DSF.

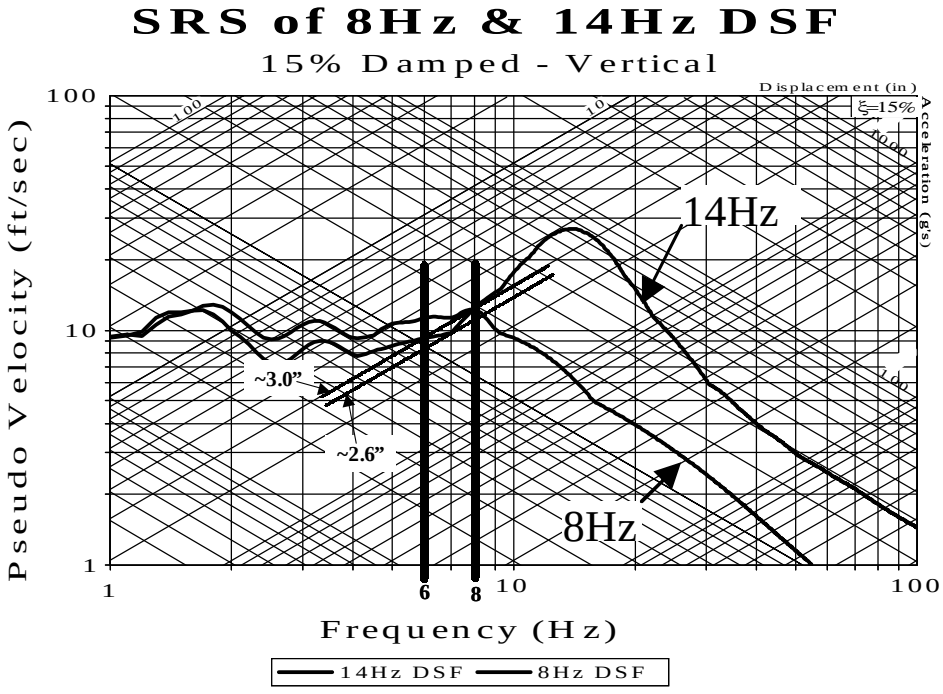

Fig. 20. SRS of 8 Hz and 14 Hz DSF.

5.1.2. Assessment of already installed cabinets using simple

After completing the SRS assessment, simulations were performed to confirm the lack of mount stroke and get a sense of the damage potential for the already installed mounting systems using SIMPLE. During simulation setup in SIMPLE, general parameters such as cabinet weight, dimensions, mass moments of inertia,

Table 2
Summary of assessment using the SRS method

No.	Units	Evans mounts	Unit Wt., [lb]	Dir	Nat'l freq [Hz]	Avail Stroke [in]	Needed Stroke [in]
1	UPS ENCL Type 2 #90–506	Base = HM08500-3 (4 ea)		X	6.22		
		Sway = HM08500-4 (2 ea)	675	Y	6.99	2.25	~ 3.6
				Z	8.69		
2	Atm Unit 3 & 5	Base = HM08375-4 (4 ea)		X	5.71		
	#90-507-1	Sway = HM08375-5 (2 ea)	500	Y	6.37	2.00	~ 3.5
				Z	7.36		
3	DAU Type 2	Base = HM08375-4 (4 ea)		X	5.76		
	#90-509-1	Sway = HM08375-5 (2 ea)	490	Y	6.43	2.00	~ 3.5
				Z	7.43		
4	BAT ENCL Type 1	Base = HM08375-5 (4 ea)		X	5.73		
	#90-513	Sway = HM08375-6 (2 ea)	370	Y	6.32	2.25	~ 3.5
				Z	7.36		
5	SOSU Type 2	Base = HM08375-5 (4 ea)		X	5.88		
	#90-503-2	Sway = HM08375-6 (2 ea)	350	Y	6.49	2.25	~ 3.5
				Z	7.55		
6	UPS ENCL Type 1	Base = HM08250-5 (4 ea)		X	6.37		
	#90-502-1	Sway = HM08250-6 (2 ea)	210	Y	6.74	1.50	~ 3.2
				Z	7.13		
7	RSOS	Base = HM08250-6 (4 ea)		X	6.11		
	#90-512-2&3	Sway = HM08250-7 (2 ea)	170	Y	6.51	1.63	~ 3.2
				Z	7.01		
8	DAU	Base = HM08250-6 (4 ea)		X	6.11		
	#90-508-X	Sway = HM08250-7 (2 ea)	170	Y	6.51	1.63	~ 3.2
				Z	7.01		
9	DAU & Battery ENCL	Base = HM08500-3 (8 ea)		X	4.73		
	#90-511-1	Sway =HM08500-4 (4 ea)	2360	Y	5.32	2.25	~ 3.3
	#90-514			Z	6.61		
10	DAU Type 2 & 4	Base = HM08375-2 (8 ea)		X	5.24		
	#90-511-1	Sway =HM08375-3 (4 ea)	1810	Y	5.90	1.65	~ 3.2
	#90-509-2			Z	7.16		
11	Triple SOSU	Base = HM06500-3 (8 ea)		X	5.18		
	#90-505-1/2/3	Sway = HM06500-4 (4 ea)	1500	Y	5.82	2.25	~ 3.2
				Z	7.19		
12	SOSU & ATM	Base = HM08375-2 (6 ea)		X	5.82		
	#90-503-1	Sway = HM08375-4 (3 ea)	1030	Y	6.47	1.65	~ 3.6
	#90-507-2			Z	8.07		
13	Double SOSU	Base = HM08375-2 (6 ea)		X	5.91		
	#90-504-1/2	Sway = HM08375-4 (3 ea)	1000	Y	6.56	1.65	~ 3.6
				Z	8.19		
14	Battery ENCL Type 2	Base = HM08500-3 (4 ea)		X	4.96		
	#90-514	Sway = HM08375-4 (2 ea)	1040	Y	5.46	2.25	~ 3.2
				Z	6.98		

mount locations, mount orientations, mount characteristics, cabinet orientation to shock, input data, and others were selected to represent the cabinet installations on a 14 Hz DSF. Vendor mount characteristics were read directly from the mount library (e.g. force-displacement curves, damping, mount height, etc) and modified to approximate the constraints of mount bottoming and topping. A schematic of the 350 lb SOSU unit, shown in Fig. 21, depicts the orientation and location of mounts as setup in SIMPLE.

Simulations using 15% Cr were run for several units to confirm bottoming & topping using the modified force displacement curves. These modifications extrapolate the vendor's data into a stiffer region (e.g. 50 Hz) that simulates the forces and displacements that occur when impacting (bottoming) or severe yanking (topping) on a structure. The resulting vertical force vs relative displacements at point L for both the applied and un-damped forces are shown in Fig. 22 for all mount loading cycles out to 2 seconds. Point L is on the SOSU unit shown in Fig. 21 at the top center of the front right base mount (looking into Y axis). Note: The parentheses around the respective letters indicate they are far in distance. The fact that the relative displacement at point L extends $\sim$3/4 inch past the point at which the mount bottoms indicates that significant

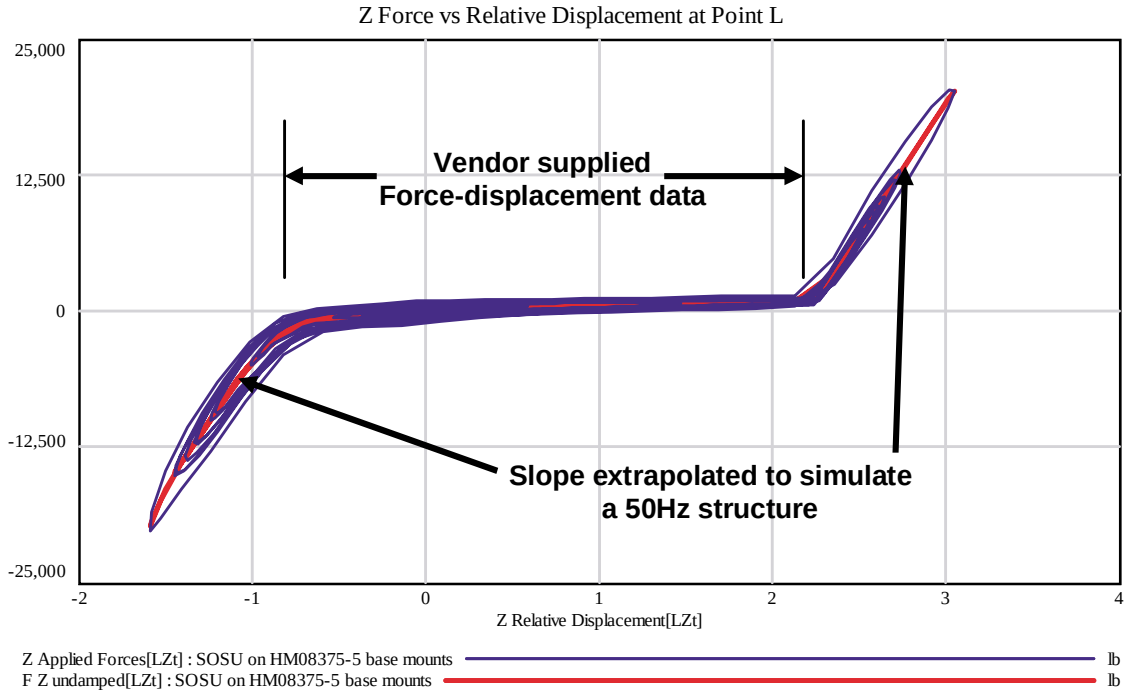

Fig. 22. SOSU Force VS Displacement at Point L.

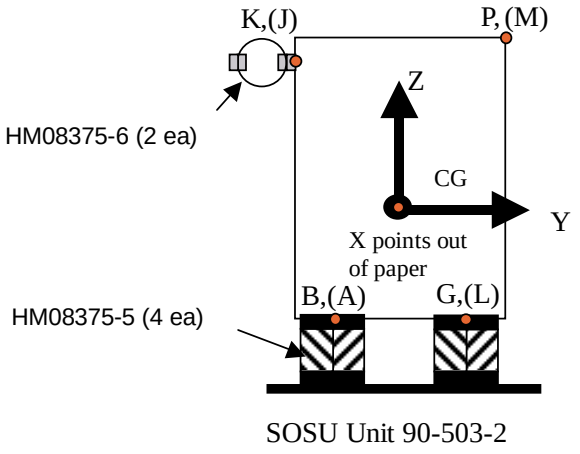

Fig. 21. Schematic of 350 lb SOSU unit.

accelerations and permanent deformation of the cabinet or even mount failure are likely to occur.

The relative displacement and acceleration time histories for point L are shown in Figs 23 and 24 respectively. The vertical or Z relative displacement in Fig. 23 shows the SOSU bottoming and topping about 17 times. The only energy loss was estimated from 15% Cr. After bottoming in compression, the system turns sharply and begins topping out in tension when it reaches approximately −1.0 inch. This is because the mount becomes as stiff as its supporting structure in tension at −1.0 inch and cannot extend beyond −1.2 inches from its unloaded position without extensive damage to the mount. The result of the bottoming and topping are excessive accelerations as shown in Fig. 24. Repeatedly exceeding the mount capacity, will increase the likelihood of cabinet and mount failure as damage [31] accumulates linearly every time the system bottoms or tops out.

5.2. *Application for design*

The purpose of this application was to provide a mount performance trade study for the Smartship Integrated Ship Controls to: 1) identify mount options meeting dynamic performance goals and 2) compare shipboard and individual cabinet interfaces associated with each mount option. Designs based on 4 vendor options were considered: DTI mounts, ShockTech Arch's, IDC wire ropes, and John Evans wire ropes. Preliminary designs for each option were developed for each of the 15 cabinets in the study for a total of 60 configurations. Then simulations were run on the 60 configurations using SIMPLE to confirm or iterate the selection, location, and orientation of mounts. Overall comparisons of the 4 options were then made. Comparisons took into account performance as well as shipboard and cabinet interfaces.

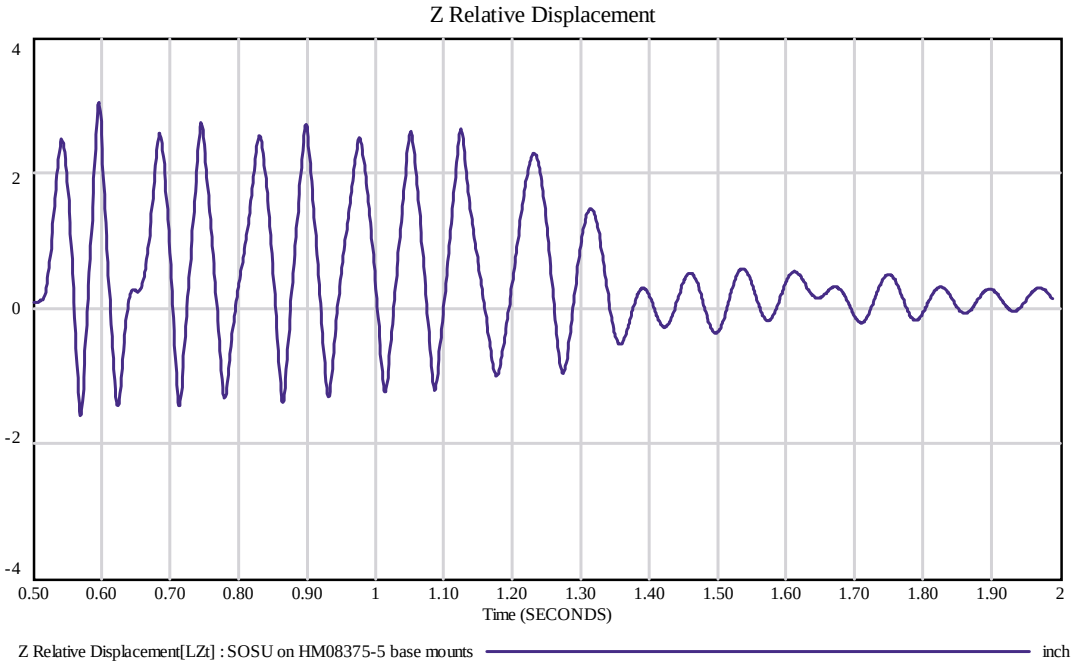

Fig. 23. Relative displacement at Point L.

5.2.1. Preliminary designs

Following the process for system design in Fig. 1, the SRS was examined to select acceptable natural frequencies for the isolation systems where the relative displacement was $<$ 3.6 inches. The previous assessment indicated the bandwidth between 6 to 8 Hz would result in acceleration levels meeting the performance goal of accelerations $<$ 25g's. However, this bandwidth applies to an unconstrained linear mount system whereas the mounts under consideration are stroke limited, non-linear, and non-symmetric. Considering these constraints, and the desire to achieve an equipment response of $\sim$20g's on the 14 Hz DSF, the nominal bandwidths for each of these mounts were determined. They are: $\sim$6.3 to 6.7 Hz for wire ropes, $\sim$5.3 to 6.3 Hz for Shocktech arches, and 7.3 to 7.7 Hz for DTI mounts.

For wire rope mounts, a frequency lower that 6.3 Hz resulted in high displacement and put at risk mounts with an available compression stroke $<$ 4 inches. If the available mount stroke was on the order of 4.5 inches, this frequency may go as low as 5.7 Hz. Wire rope systems with frequencies $>$6.7 Hz would result in more displacement on the much stiffer tension side of the mount. This would cause the acceleration level to go beyond the desired 20 g level. In addition, the available stroke in tension is about half that in compression. For these reasons, the best practice when designing systems with helical wire rope mounts is to use as much of the compression stroke as possible without risking bottoming. Doing so reduces the amount of stroke in tension and thus minimizes the system acceleration when in tension.

Using the nominal bandwidths described above, mounts and the orientation of their principal axes on the cabinets were determined. This was done using the system weight and stiffness values derived from the mount force-deflection curves using Eq. 11. Mounts were then configured to accommodate foundation and cabinet interfaces and minimize moments. Figure 25 shows a comparison of configurations for the UPS Enclosure Type 1. From left to right are configurations with DTI mounts, Shocktech arches, IDC and Aeroflex wire ropes, and John Evans Wire ropes. In a similar manner, each of the 15 units were sized with four different mount configurations for a total of 60 configurations altogether.

5.2.2. 6DOF analysis using simple simulations and results

Each configuration for the 15 units was modeled and simulated in SIMPLE and predictions were made for the corner points of each unit as shown in Fig. 26. Inputs used for predictions were the vertical, athwartship, and rotational motions of a 13 Hz DSF during a test

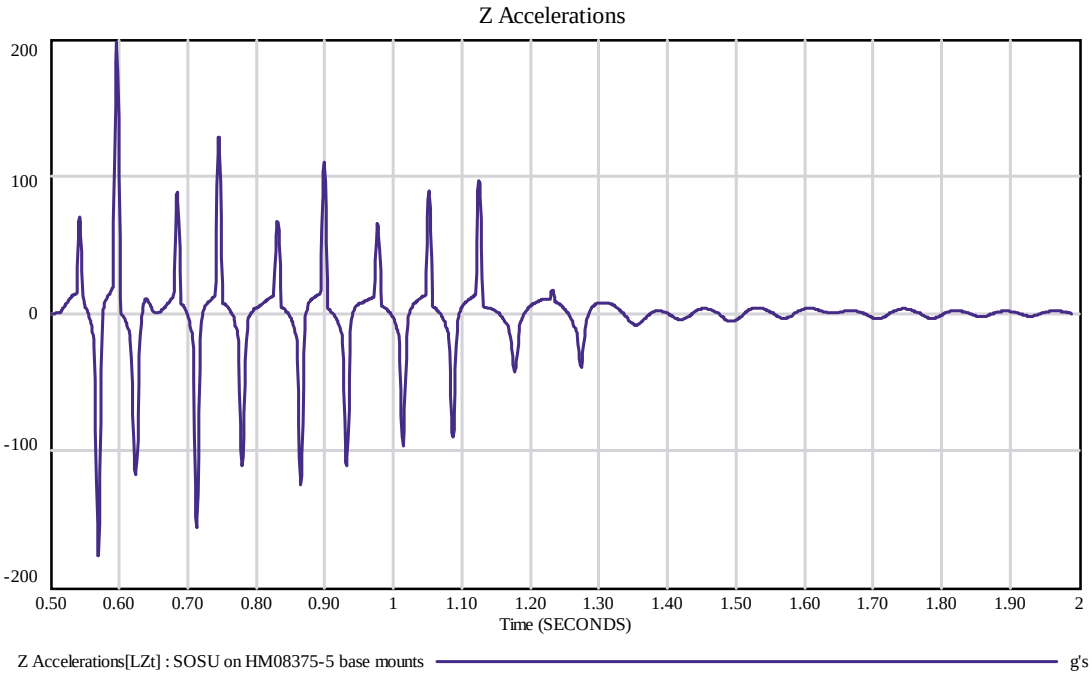

Fig. 24. Acceleration at Point L.

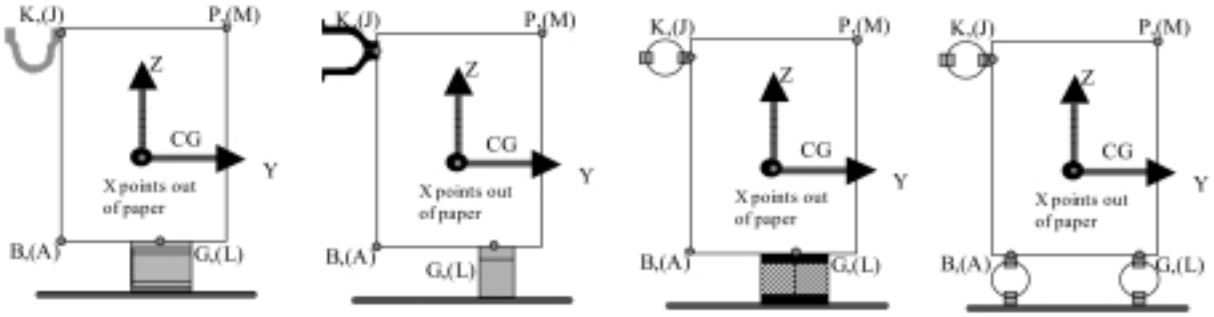

Fig. 25. Mount options for the UPS Enclosure Type 1.

with the charge at a horizontal standoff of 20 ft. For each unit, three orientations were simulated: side-to-side (Athwartship directed along +X), back-to-front (Athwartship directed along +Y), and front-to-back (Athwartship directed along −Y). This provided the results of 180 simulations to perform an assessment of the 15 units in un-restricted orientations. For each of these orientations, the units were located on the blast side of the DSF as depicted in Fig. 6. This position on the DSF corresponds to the location of the most severe input. A summary of the acceleration responses and impact of the mounts on the cabinet and ship interfaces are presented in Table 3. These responses are based on rigid body approximations for the cabinets. However, slightly higher accelerations were expected during shock testing due to excessive motion of cabinet components such as batteries, power supplies, internal chassis', and cabinet doors which had inadequate or flexible restraints. For those cases, having a cabinet system to mount system stiffness ratio at least 10:1 is unlikely.

A trade study was performed using the 60 configurations and several other evaluation factors such as schedule, cost, ease of back-fit, etc. DTI configurations were eventually selected for testing. Excursions predicted for the 15 units on DTI mounts included both the static and dynamic relative displacements at each of the corner points shown in Fig. 26. Maximum and minimum values at each of the corner points for each of the simulations were determined. Next, the worst

Table 3
Summary of mount accelerations and interface issues

Item	DTI mounts	ShockTech arch mounts	IDC mounts	John evans mounts
Natural frequency range for optimum response on 14 Hz DSF	7.3 to 7.7 Hz. in compression or tension	5.3 to 6.3 Hz in compression only	6.3 to 6.8 Hz in compression only	6.3 to 6.8 Hz in compression only
Response range predicted with SIMPLE Simulations	∼18–21g's	∼15–20g's	∼18–20g's	∼18–21g's (one case was about 30g's in tension)
Impact on existing cabinet interface	None	Must re-design for 2 units	Must re-design interface for ganged units Sway brace brackets need to be made flush with units Interference of wire rope mounts with cable way	Same as IDC mounts

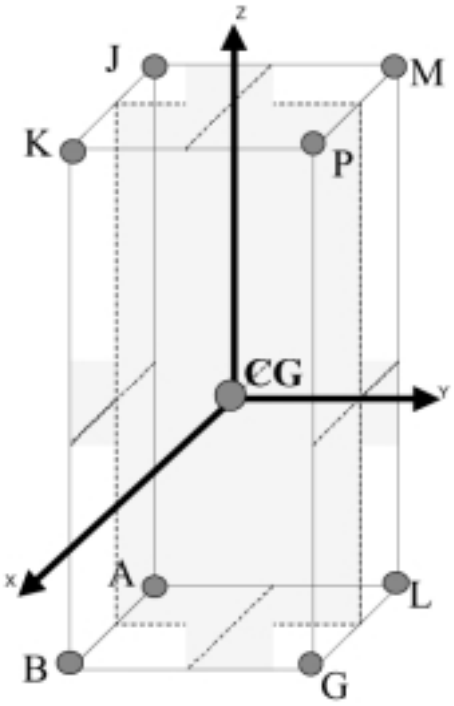

Fig. 26. Prediction locations.

case values were identified to determine the overall excursion space needed for each unit. Table 4 shows the summary values for all orientations. These values have opposite signs (e.g. –2.3 inches for Z relative displacement is interpreted as the unit moved 2.3 inches in the positive Z direction during shock). This convention was adopted to make comparisons with accelerations that are 180 degrees out of phase with relative displacement. The largest vertical displacements are 3.6 inches downward and 3.1 inches upward and the largest lateral displacements are 3.3 inches front-to-back and 3.0 inches side-to-side. Based on these values and the uncertainty of the shipboard environment, the recommended excursion envelope for DTI mounted systems on the ship should be at least 4 inches all around (e.g. up, down, front-to-back, and side-to-side).

5.3. Assessment of effeciency

An average of 1 hour per mount system was expended to build and simulate models for each of the 60 configurations. This did not include time required for gathering information and developing the preliminary designs. However, it did include time required to iterate the design to obtain acceptable responses. This short time frame for modeling and simulating was possible as a result of the following features in SIMPLE: 1) the ability to obtain all of the necessary mount properties by selecting the mounts from a library; 2) ability to select shock test inputs directly from a menu; 3) ability to orient the unit with respect to the input by setting a rotation angle; and 4) ability to easily make changes to all modeling parameters in the SIMPLE template by clicking on them and entering new values for simulation. Therefore, the case has been made that the hypothesis is true and 6DOF simulation methods can be made practical and efficient. Questions 3 and 4 regarding the sensitivity and validity of responses associated with simplifying the specification of these parameters are addressed in the next section.

6. Analysis of test results

SIMPLE is also a tool that can easily account for uncertainties in isolated systems and their environments.

Table 4
Worst case maximum and minimum responses for each direction in all orientations

Relative Displacements		Worst case max & min responses														
		UPS ENCL Type 2 [in]	Atm Unit 3 & 5 [in]	DAU Type 2 [in]	BAT ENCL Type 1 [in]	SOSU Type 2 [in]	UPS ENCL Type 1 [in]	UPS ENCL Type 1A [in]	RSOS [in]	DAU [in]	DAU & Battery ENCL [in]	DAU Type 2 & 4 [in]	Triple SOSU [in]	SOSU & ATM [in]	Double SOSU [in]	Battery ENCL Type 2 [in]
X direction	Min	−2.5	−2.5	−2.8	−2.2	−2.7	−2.1	−1.2	−1.6	−1.8	−1.5	−1.5	−1.4	−1.7	−1.9	−1.7
	Max	2.7	2.5	2.3	2.1	2.5	2.0	1.0	1.5	1.8	1.6	1.3	1.3	1.5	1.8	3.0
Y direction	Min	−2.6	−2.6	−2.7	−1.8	−2.6	−1.8	−0.7	−2.2	−2.0	−3.1	−2.6	−2.6	−2.2	−3.2	−3.1
	Max	1.5	1.7	3.3	2.5	2.3	2.5	1.3	3.0	2.7	1.4	3.2	2.5	2.6	1.6	1.4
Z direction	Min	−2.4	−2.5	−2.5	−2.8	−2.3	−3.1	−1.1	−2.3	−3.0	−2.6	−2.4	−2.4	−2.6	−2.3	−2.6
	Max	3.2	3.2	3.2	3.0	3.2	3.1	1.7	3.6	3.2	3.3	3.2	3.2	3.2	3.3	3.2

In this section, experimental results from shock tests are compared with pre-test SIMPLE sensitivity simulations and with results of post-test model calibrations. These comparisons show the validity of: 1) using 6DOF analysis; 2) using statically derived load-deflection data for simulations; and 3) assessing and designing isolated systems using uncertainties in model parameters.

6.1. Using 6DOF analysis to assess coupled modes

The responses of some of the systems where SIMPLE was applied in the design are shown in Figs 27 and 28. Figure 27 depicts the vertical acceleration measured just above the shock mounts on each unit and Fig. 28 shows the SRS of these responses compared to the input.

Figure 27 shows that all units except the Battery Enclosure, met the desired performance requirement of ∼25g's. The higher g's in tension for the Battery Enclosure may be a result of the loss of impedance from internal components (e.g. batteries) when the cabinet motion reverses. Although the acceleration goal was not met for the Battery Enclosure, it remained operational during shock was subsequently shock qualified.

Figure 28, which compares the SRS of the DSF input with those of the units, indicates that all of the units are significantly responding between 6 to 8.5 Hz. These frequencies are likely responses of coupled modes. For example, consider the response at the center of gravity of the rigid body system with one plane of symmetry shown in Fig. 15. This system experienced input along two axes similar to the units tested here and had a calculated vertical (in the Z direction) natural frequency of 7.22 Hz. However, due to coupled modes, the resulting frequencies that were observed were 6.02 Hz and 9.75 Hz as shown in Fig. 16. The actual natural frequency of the system (e.g. 7.22 Hz) coincided with a dip between these two values.

Recall that the vertical natural frequencies used in the design process for DTI mounted systems ranged from 7.3 to 7.7 Hz and are based on stiffness values calculated by Eq. 11, which uses the mount static load-deflection curves. Finding these values in the SRS for each of the units may be difficult due to the coupled modes. This is illustrated in Fig. 29, which shows the ratios of the responses of the mounted systems listed in Fig. 28 to the input measured at the center of the DSF. Since the input of the DSF varies across the surface, the ratios do not represent the true transmissibility of the systems. As with the one plane of symmetry system, the calculated natural frequencies appear to coincide with the dips between the coupled modes. This dip phenomenon at the natural frequencies also occurs in other simulated systems where coupling occurs. For uncoupled systems, the maximum response will occur at the natural frequency of the system. However, for isolated shipboard euipment with multiple input scenarios, coupled modes will predominate. To address the coupled mode issues, practical 6DOF analyses such as that provided by the SIMPLE simulation method are needed.

6.2. Using statically derived load-deflection data

SIMPLE was used to confirm the design of a wire rope system for a VMS console. The calculated natural frequency in the Z direction for the console was 6 Hz. This frequency also coincides with the dip between the coupled modes as shown in Fig. 29. If the natural frequencies occur only in the dips of the coupled systems shown in Fig. 29, then the ratio of dynamic to static stiffness for DTI and wire rope mounts would have to be close to unity for shock related events. This agrees with Hain and others [17].

Static load-deflection curves show that many mounts are stiffer at small displacements. As a result, the expectation is that vibration responses will occur at higher

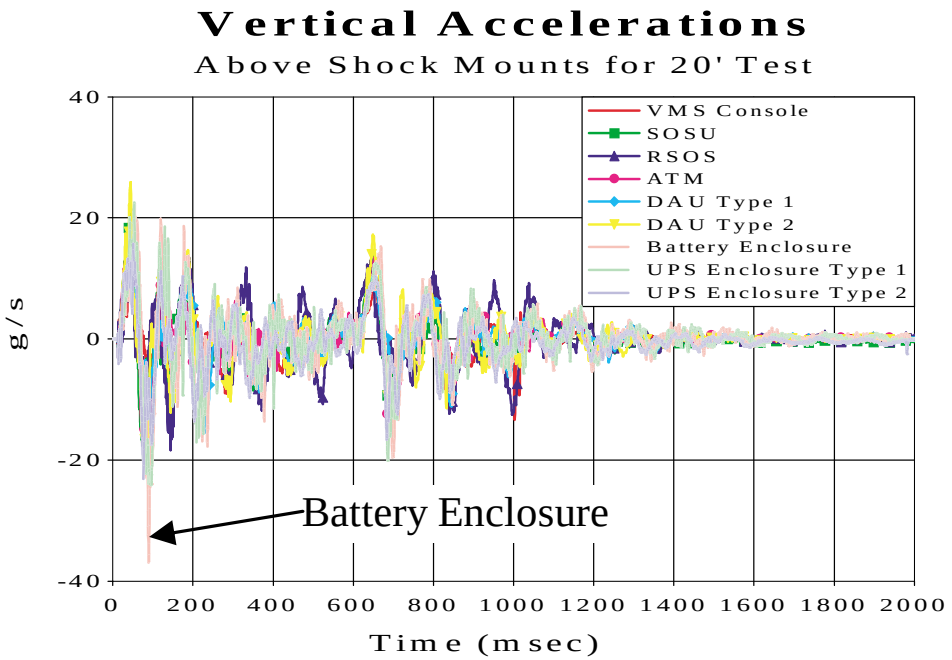

Fig. 27. Vertical accelerations measured above shock mounts.

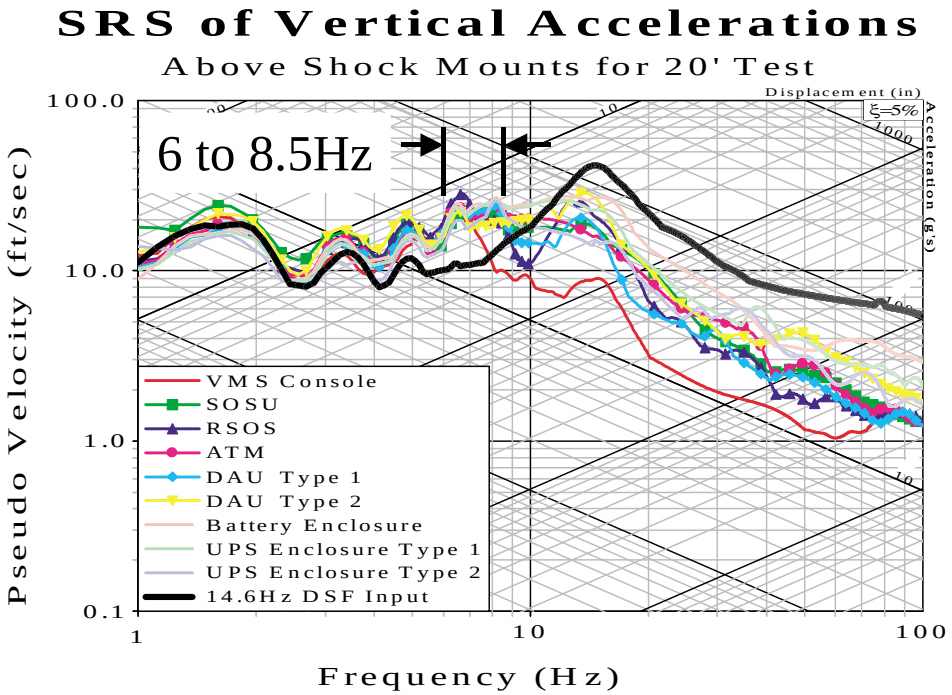

Fig. 28. SRS of vertical accelerations above mounts compared to DSF input.

frequencies than shock responses. Figure 30 shows a comparison of shock [26] and vibration [32] responses occurring on a unit know as the ATM Switch. Unidirectional input during vibration testing resulted in significantly less coupling than shock responses. As a result, the maximum vibration responses coincided very

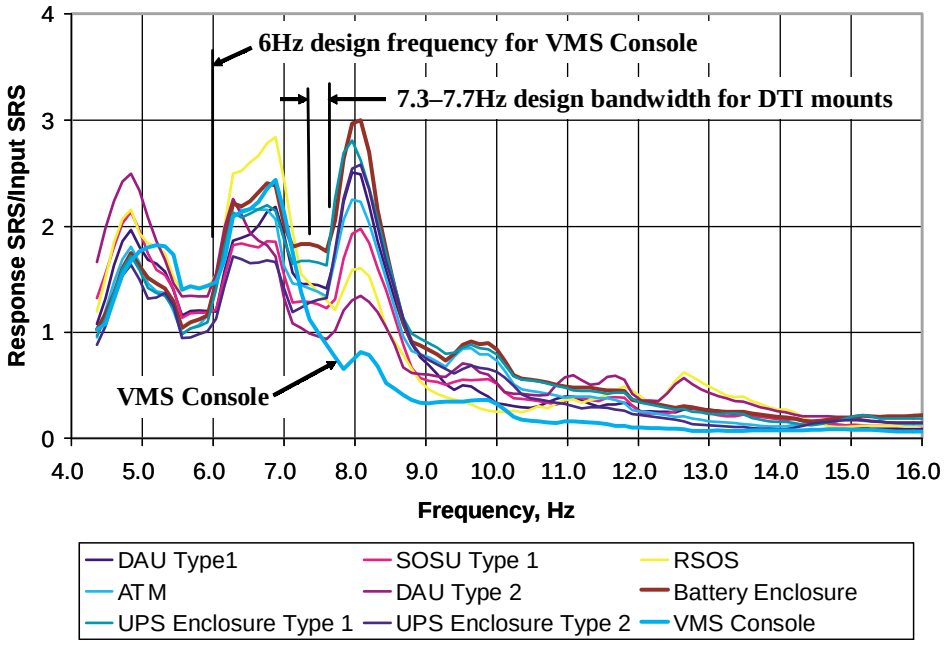

Fig. 29. Response to input ratios for mounted systems on a 14.6 Hz DSF.

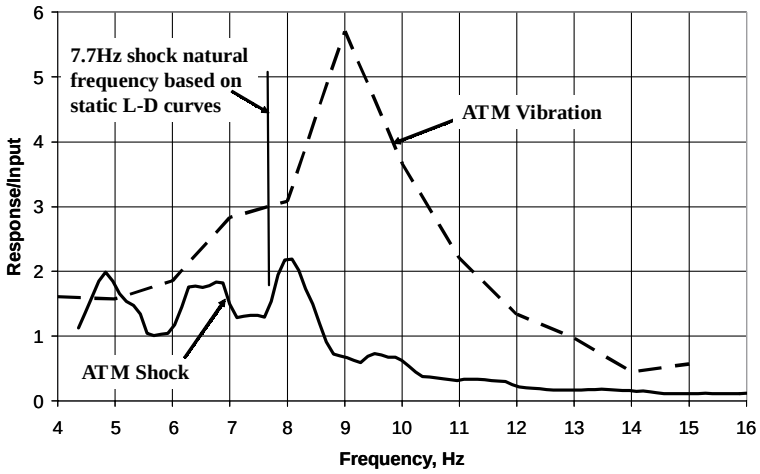

Fig. 30. Comparison of shock and vibration responses of the ATM Switch.

near to the natural frequencies of the systems at small displacements. Shock responses on the other hand resulted from multiple inputs of considerable severity in the vertical and lateral directions. The ATM Switch has a calculated shock frequency of 7.7 Hz for ∼3 inch displacements in accordance with Eq. 11. However, static load-deflection curves for DTI mounts at vibration level displacements (e.g. less that 0.4 inches) show an increase in stiffness of 1.3 to 1.5 that of the shock stiffness. Therefore, as Fig. 30 shows, the natural frequency of the ATM unit will change from 7.7 Hz to ∼9 Hz during vibration testing. A review of vibration results of all the DTI mounted systems show maximum responses occurring at frequencies between 8.5–9.5 Hz in the Z direction. This also suggests that little if any dynamic stiffening is occurring in the DTI mounts.

6.3. Using uncertainties in model parameters

In order to answer question 3, comparison of predicted and experimental data via sensitivity analysis is presented in this section for the SOSU Type 2 unit.

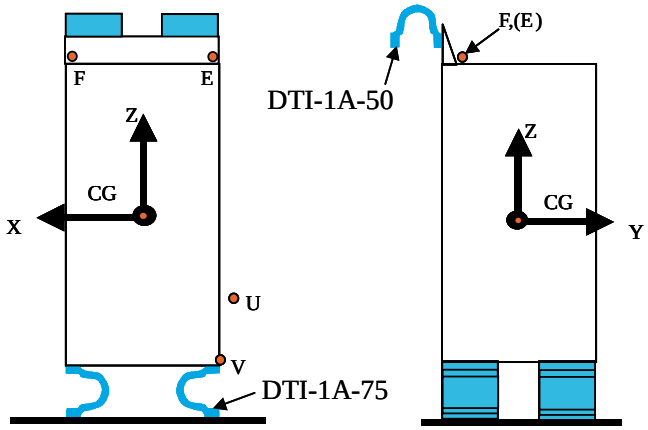

Fig. 31. SOSU Unit showing mount and measurement locations.

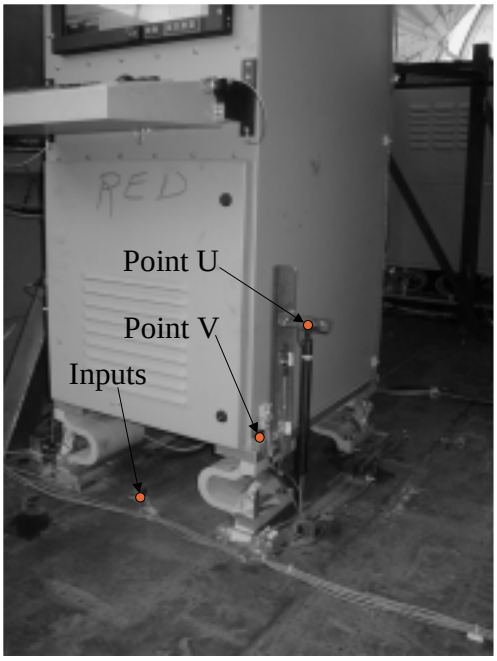

Fig. 32. SOSU measurement locations at the base.

Performing sensitivity analyses with the SIMPLE simulation template involves: 1) specifying distributions that represent the uncertainties in the values of model parameters; 2) selecting the number of simulations; and 3) deciding whether to vary one parameter at a time of all of them together (multivariate). For the SOSU sensitivity analysis, 200 simulations were run and 30 parameters were varied in multivariate mode. Of the 12 types of distributions to choose from in SIMPLE, random uniform was selected for each parameter so that sampling over the specified range of values would be equally likely.

Each parameter varied for the SOSU analysis and the minimum and maximum values for their distributions (specified in parentheses) are listed below. The first six parameters in the list vary the scale of the load deflection curves by +or- 20% for the base [mount 1] and sway mounts [mount 2] depicted in Fig. 31. This allows effects such as dynamic stiffening and/or mount degradation to be included in the analysis. Parameters 7–12 vary the percent critical damping between 5–10% at each mount location. Parameters 13–15 account for the uncertainty in the location of the cabinet's center of gravity and parameters 16–25 specify the uncertainty for the inertial properties of the system such as the inertia tensor and cabinet weight. The uncertainty of where the unit is mounted with respect to the reference frame is accounted for by parameters 26 and 27. And finally the uncertainty in rotational and vertical input is specified by parameters 28, 29, and 30.

1 CT Mount scale factor[Mount 1]= RANDOM_UNIFORM(0.8,1.2)
2 CT Mount scale factor[Mount 2]= RANDOM_UNIFORM(0.8,1.2)
3 ROLL Mount scale factor[Mount 1]= RANDOM_UNIFORM(0.8,1.2)
4 ROLL Mount scale factor[Mount 2]= RANDOM_UNIFORM(0.8,1.2)
5 SHEAR Mount scale factor[Mount 1]= RANDOM_UNIFORM(0.8,1.2)
6 SHEAR Mount scale factor[Mount 2]= RANDOM_UNIFORM(0.8,1.2)
7 CT percent Cr[MOUNT 1 percent Cr3]= RANDOM_UNIFORM(0.05,0.1)
8 CT percent Cr[MOUNT 2 percent Cr3]= RANDOM_UNIFORM(0.05,0.1)

9 ROLL percent Cr[MOUNT 1 percent Cr1]=
RANDOM_UNIFORM(0.05,0.1)
10 ROLL percent Cr[MOUNT 2 percent Cr1]=
RANDOM_UNIFORM(0.05,0.1)
11 SHEAR percent Cr[MOUNT 1 percent Cr2]=
RANDOM_UNIFORM(0.05,0.1)
12 SHEAR percent Cr[MOUNT 2 percent Cr2]=
RANDOM_UNIFORM(0.05,0.1)
13 X' cg=RANDOM_UNIFORM(11,13)
14 Y' cg=RANDOM_UNIFORM(16,18)
15 Z' cg=RANDOM_UNIFORM(27.5,29.5)
16 Cabinet Ix if provided=
RANDOM_UNIFORM(290,390)
17 Cabinet Iy if provided=
RANDOM_UNIFORM(250,350)
18 Cabinet Iz if provided=
RANDOM_UNIFORM(80,180)
19 Pxy if provided=
RANDOM_UNIFORM(−50,50)
20 Pxz if provided=
RANDOM_UNIFORM(−50,50)
21 Pyx if provided=
RANDOM_UNIFORM(−50,50)
22 Pyz if provided=
RANDOM_UNIFORM(−50,50)
23 Pzx if provided=
RANDOM_UNIFORM(−50,50)
24 Pzy if provided=
RANDOM_UNIFORM(−50,50)
25 CABINET WEIGHT=
RANDOM_UNIFORM(350,380)
26 CG distance to reference frame[CG ref X coord]
=RANDOM_UNIFORM(−30,57)
27 CG distance to reference frame[CG ref Y coord]
=RANDOM_UNIFORM(30,50)
28 scale for DSF deformation rotation=
RANDOM_UNIFORM(0.5,1.5)
29 scale for Ref Angular Velocity about Y=
RANDOM_UNIFORM(0.5,1.5)
30 Z Input Scale Factor=
RANDOM_UNIFORM(0.8,1)

Results of the sensitivity simulations were compared with SOSU test data for the locations shown in Figs 31,32 and 33. Accelerometers are located at Points F and V and displacement gages are located at Points E and U.

Figures 34,35,36,37,38 show the SOSU sensitivity results where 95% confidence bounds for the response at each point is compared to test data. These results confirm the hypothesis that reasonable predictions for isolated systems can be made even in the presence of uncertainties. This provides designers the ability to identify parameter constraints and assess their effect on the responses of the system. For example, consider the weight, mass moments of inertia, and center of gravity of a cabinet, which may vary considerably during cabinet design and development while the spatial constraints for mounting interfaces (e.g. shipboard arrangements and foundations) remain constant. Using the sensitivity feature in SIMPLE allows the designer to identify acceptable constraints for these parameters that do not adversely affect dynamic responses.

6.4. Calibration using test data

Post-test calibration of models is useful when baseline cabinet configurations are needed to more accurately assess: 1) cabinet responses at different locations and 2) changes that may occur during the life cycle of the cabinet. These changes may include addition of heavier or lighter sub-components during equipment upgrades; placement of an identical or modified cabinet in a different shock environment; relocation of mounts; etc.

After calibration of models, sensitivity analyses can be performed on the calibrated configurations. This sensitivity assessment is different from what was previously discussed in that the isolated system responses are constrained to acceptable values while searching over the model parameters to find variances that are acceptable. This is done to determine how much each individual parameter may be changed within the response constraints. The values over which each parameter may assume and still achieve valid responses represents the range of validity of each parameter.

A modified Powell optimization search technique [20] is used for calibration. At each time step in the simulation, the difference between the data and the model variable is multiplied by the specified weight and this product is then squared. This number is then subtracted from the payoff so that the payoff is always negative. Optimization occurs when the payoff is as close to zero as possible. A fractional tolerance may also be specified to determine when to terminate the optimization. Sensitivity assessments, using the calibrated or optimized model, may then be done to determine confidence intervals for the parameters. When the weights on each of the variables in the payoff are set to be proportional to the reciprocal of the standard deviation of the prediction error, the 95% confidence intervals may be obtained. This results when a change of 4 in the value of the payoff occurs. An example of the calibra-

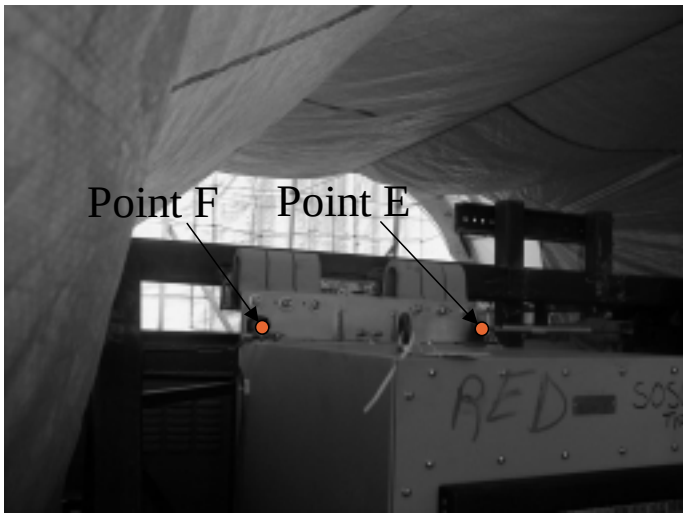

Fig. 33. SOSU measurement locations at sway locations.

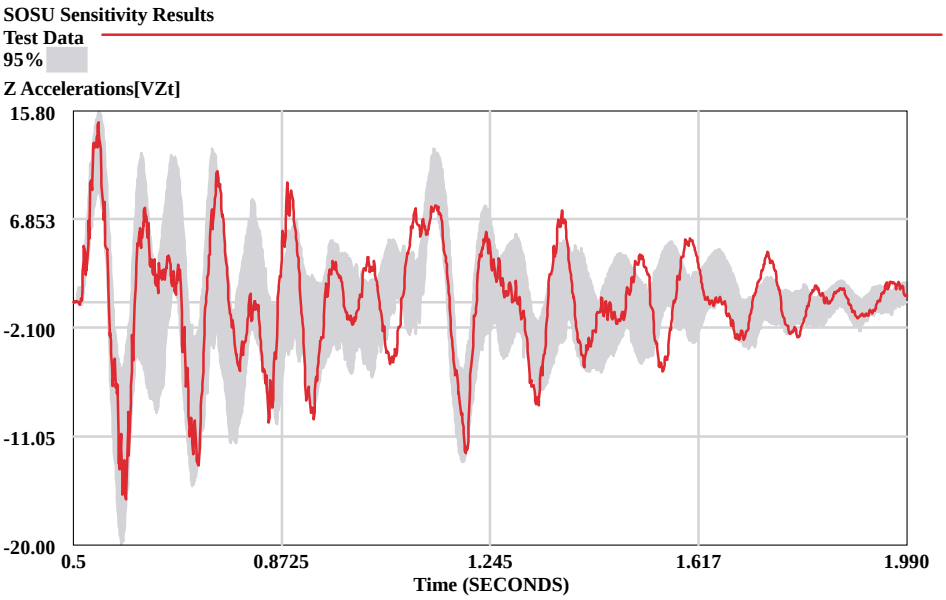

Fig. 34. Z acceleration at Point V.

tion method used in SIMPLE is presented for the SOSU Type 2 unit shown in Figs 31, 32, and 33. The same 30 parameters used in the sensitivity analysis are used in the modified Powell search. Actual measurements at the SOSU unit foundations were used for the X and Z inputs and the above mount responses were used in the calibration payoff definition. The inputs were also augmented with rotations about the X axis in accordance with Eqs 9 and 10. Comparisons of the experimental data with the predicted calibration results are shown in Figs 39 to 43. These comparisons show good agreement overall and answer question 4 by showing the validity of SIMPLE predictions when simulating with multi-axis inputs from DSFs.

The initial experimental acceleration responses shown in Fig. 39 and 40 are slightly higher than the predicted responses even after calibration. On the other hand, the predicted relative displacements in both the X and Z directions appear to be very close to the experimental values. This may be due to excitation in the above mount structure and components, which may amplify the acceleration responses of the cabinet. Rigid

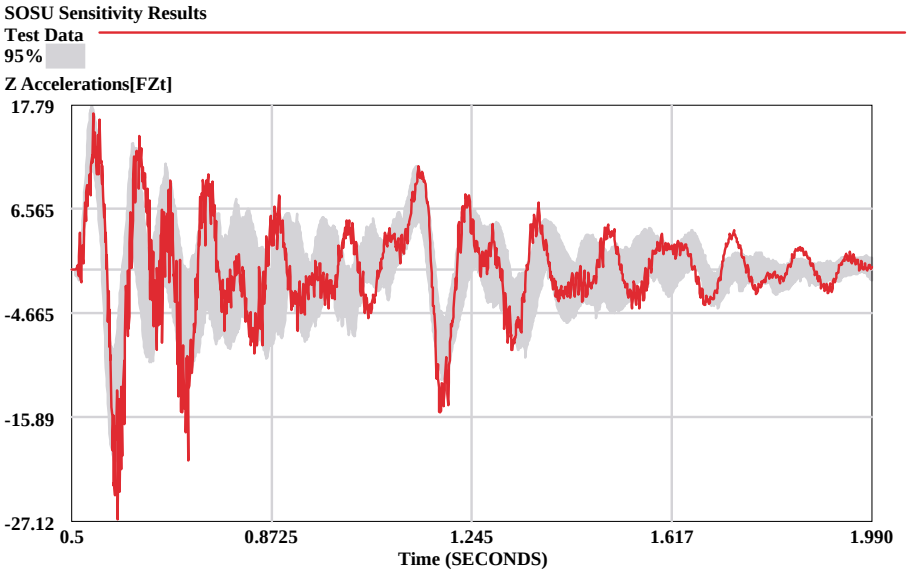

Fig. 35. Z acceleration at Point F.

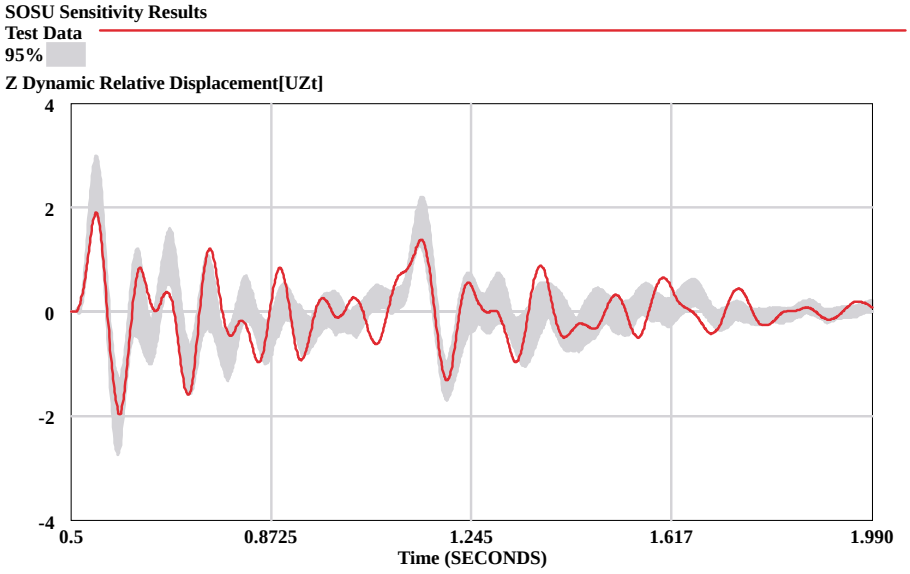

Fig. 36. Z relative displacement at Point U.

body theory does not account for relative motion of these items. Therefore, flexible or inadequate fasteners that hold down cabinet doors, battery trays, circuit card chassis' and other items such as un-interruptible power supplies may produce responses higher than rigid body theory will predict. For example, during exploratory and variable frequency vibration testing [25] of the SOSU unit, excessive responses were observed at 14 Hz on a circuit card chassis inside the SOSU cabinet. These frequencies are near the sustained frequency of the DSF and according to the Octave rule [10], they will most likely amplify the responses.

7. Conclusions and recommendations

7.1. Conclusions

The conclusion of this research is that 6DOF simulation methods can be made practical, efficient, and easy

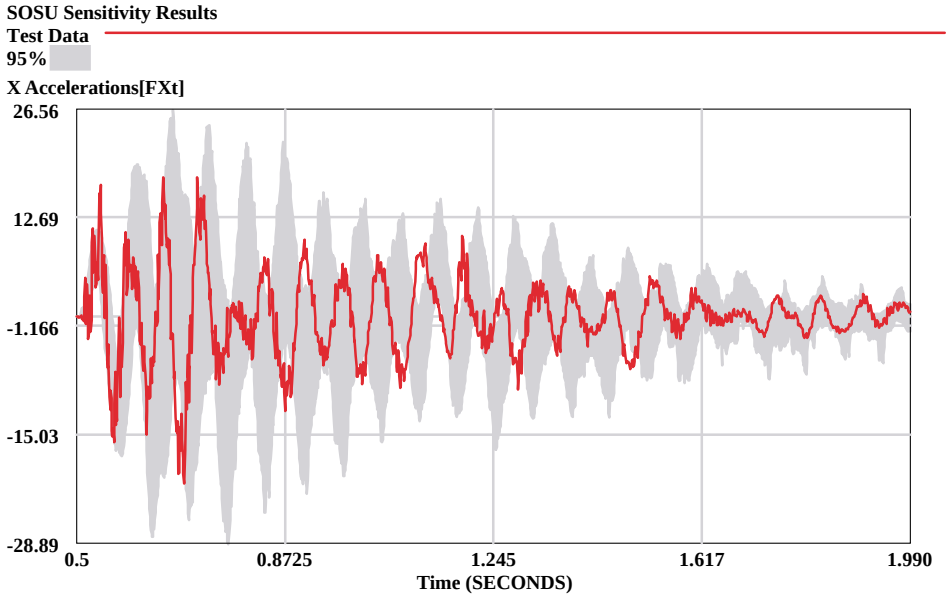

Fig. 37. X acceleration at Point F.

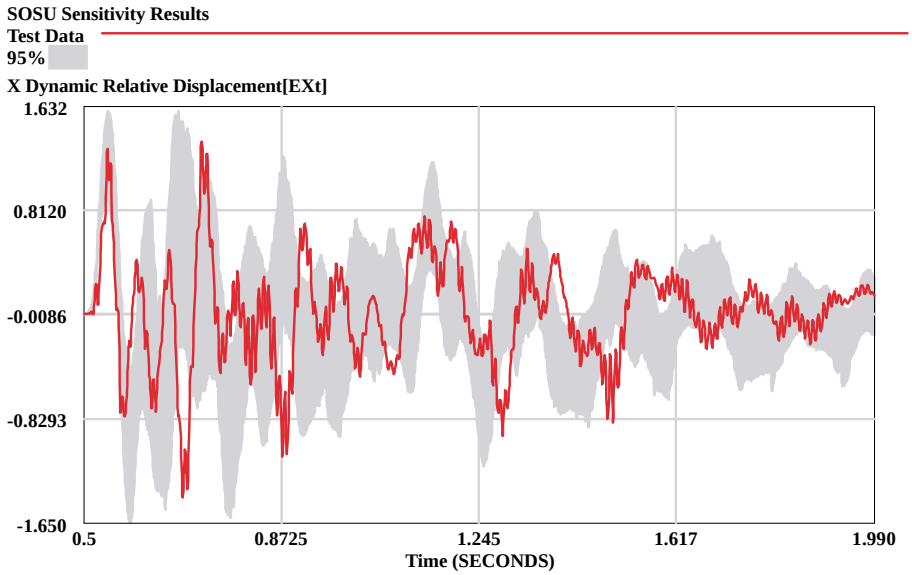

Fig. 38. X relative displacement at Point E.

to use by simplifying the specification and implementation of the many parameters used in analyzing isolated systems. Developing, validating, and applying a new, efficient, easy to use 6DOF simulation method known as Shock Isolation Mount Predictions & Loading Estimates (SIMPLE) led to this conclusion. The SIMPLE method was applied in the context of a process for assessing and/or designing shock isolation systems. The process is divided into two phases: 1) analysis using the classic [7] SRS or other methods and 2) assessment, confirmation, iteration or comparison of designs using the SIMPLE simulation method.

The process was applied to provide rapid assessments and designs (including simulations) for over 60 different mounting systems supporting the Smartship Integrated Ship Controls for CG 47 Class ships. An average of 1 hour per mount system was expended to build and simulate models for each of the 60 configura-

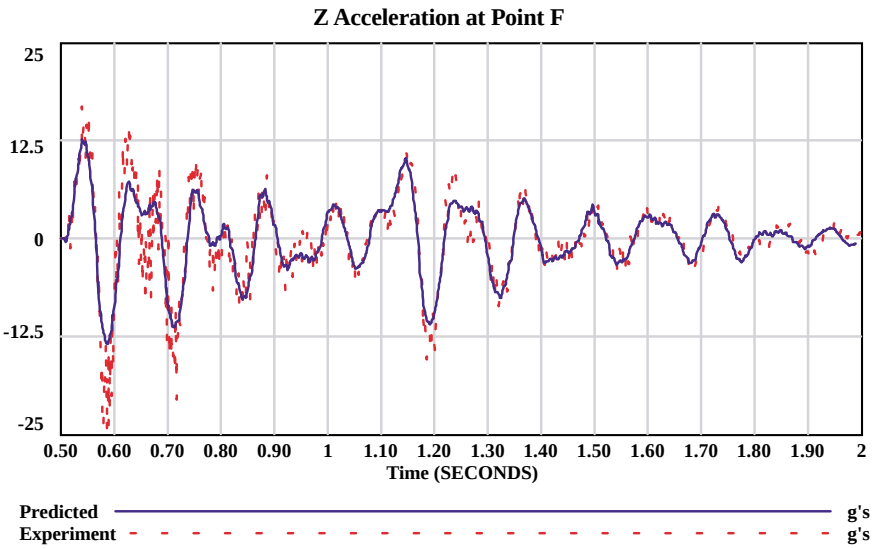

Fig. 39. Calibration results for Z acceleration at Point F.

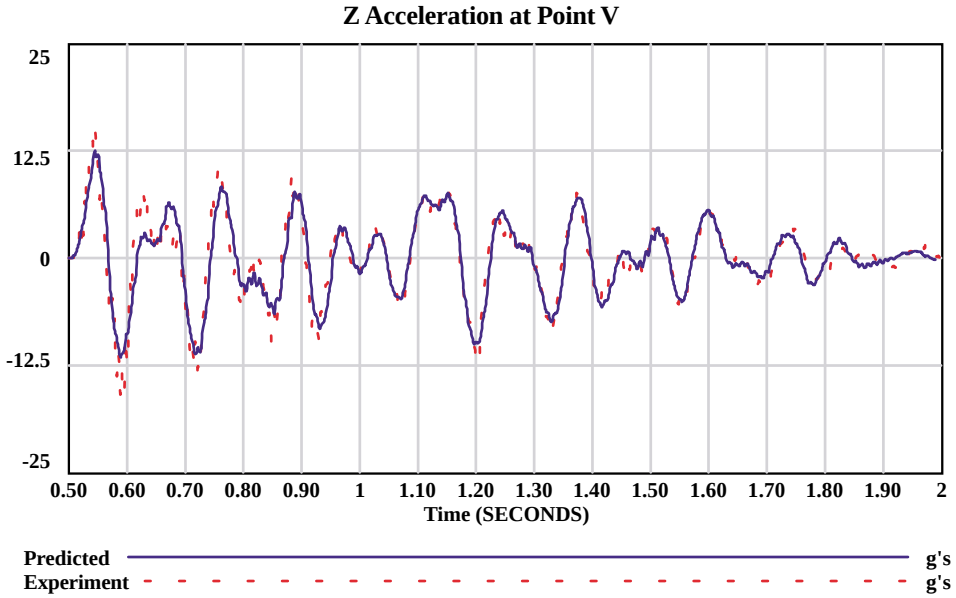

Fig. 40. Calibration results for Z acceleration at Point V.

tions. This included time required to iterate the designs to obtain acceptable responses. It did not include time required in the initial phase of the process for gathering information and developing the preliminary designs.

The applications included: 1) an assessment of existing wire rope mount systems for cabinets on two CG 47 Class Smartships; 2) a mount performance trade study with different mounting options for each cabinet; and 3) determination of excursion space and acceleration levels for each mounting system selected for testing. The SIMPLE predictions for vertical responses on the blast side of the DSF were 18–21 g's for acceleration and 3.2–3.6 inches for relative displacements. The mount performance goals were to achieve cabinet acceleration levels around 15 to 25g's with excursion envelops less than 4 inches. With the exception of one Battery Enclosure mounting system, these performance goals were met during shock tests conducted [26–28]

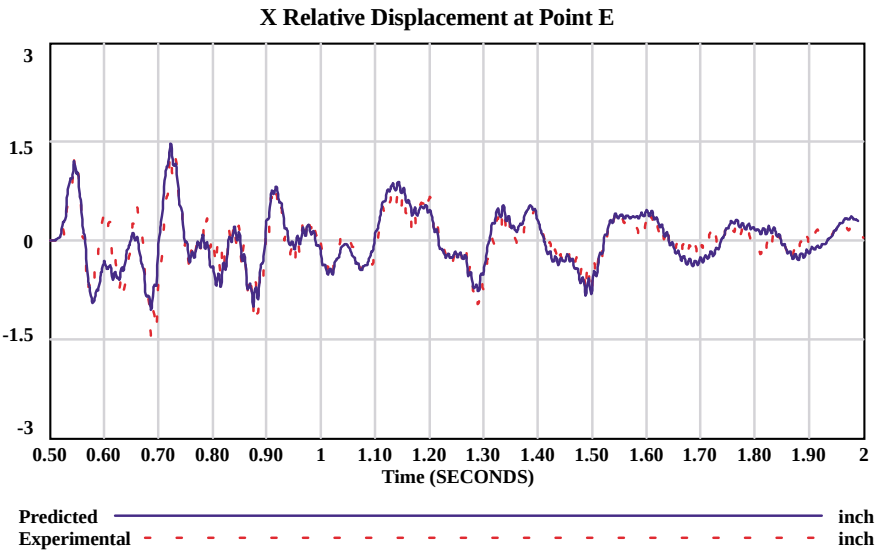

Fig. 41. Calibration results for X relative displacement at Point E.

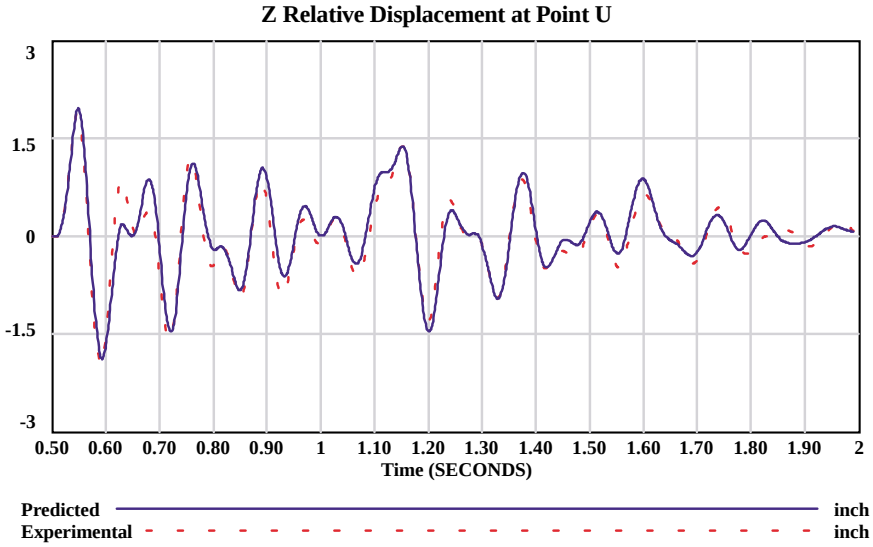

Fig. 42. Calibration results for Z relative displacement at Point U.

from December 2001 to May 2002 at HI-TEST LABORATORIES, INC. in Arvonia, Virginia. The range of measured accelerations were 15–26g's and depended on the unit location on the DSF and relative motion of cabinet components such as batteries, power supplies, internal chassis', and cabinet doors which had inadequate or flexible restraints. Meeting these performance goals contributed significantly to shock qualification of these cabinets, all of which were successfully installed aboard ship, and validated the use of SIMPLE as a design tool for isolated systems.

SIMPLE was developed specifically to address the need for practicality and efficiency in analyzing isolated systems. It provides: 1) estimates of the excursion space needed for dynamic travel of mounted systems; 2) rapid prediction of responses such as acceleration, velocity, force, displacement, etc.; 3) a design tool for the location, sizing, and orientation of mounts for equipment and structures; 4) calibration via optimization; 5) multivariate sensitivity analyses of system parameters; 6) a shock mount library of more than 250 mounts; 7) inputs from floating shock platforms, deck

simulators; medium weight shock test machines, etc.; and 8) immediate presentation of data after simulation.

Several questions regarding the use of SIMPLE as a simulation method for assessing shock and vibration were addressed. These are: 1) What kind of simplifications can be made to make the simulation method efficient and easy to use? 2) What advantage does SIMPLE have over other analysis methods? 3) How sensitive are response predictions to model parameters such as those that characterize the mounts, their location, and the inertial properties of the rigid body? 4) What is the validity of SIMPLE response predictions when simulating with multi-axis inputs from deck simulator fixtures (DSFs); floating shock platforms (FSPs), medium weight shock machines (MWSMs) and others?

In addressing question 1, it was determined that the most significant simplification is to consider the isolated cabinet or structure to be a rigid body. According to Racca [9], rigid body analysis is applicable where the foundation and isolated structure is at least 10 times stiffer than the mount. This applies to many shock isolation systems, especially those for [5,10] electronic equipment on ships and submarines. The 10:1 stiffness ratio assures that at least 90% of the isolation is from the mounts and 10% is from the structure. The resulting ratio of structure to mount system natural frequencies is $\sim$3.2:1.0.

In addressing question 2, deficiencies of existing engineering methods were examined. These include: 1) no consideration for rotational effects; 2) lack of ability to easily change parameters; 3) lack of ability to account for variances; 4) they require considerable knowledge to use; 5) they overcomplicate the modeling assumptions necessary to obtain acceptable estimates of acceleration levels & displacements, and 6) they are difficult to calibrate. It was determined that the main advantage of the SIMPLE method is that it provides comprehensive solutions to the above issues in a practical, efficient, easy to use manner.

In addressing questions 1 and 3, it was shown that SIMPLE can easily account for uncertainties in isolated systems and their environments. For example, experimental results from shock tests were compared with pre-test SIMPLE sensitivity simulations and with results of post-test model calibrations. These comparisons showed the validity of: 1) using 6DOF analysis; 2) using statically derived load-deflection data for simulations; and 3) assessing and designing isolated systems using uncertainties in model parameters.

In addressing question 4, the theory base of the SIMPLE simulation method was presented where the coupling of 3 translational and 3 rotational degrees of freedom was accomplished through the calculation of point velocities (e.g. Eq. 5). The coupling resulted in a 6DOF model that was validated by comparing SIMPLE simulation results with other analytical methods that included multi-axis inputs. Additional validation was performed using multi-axis inputs from a DSF.

7.2. Recommendations for future research

To better address questions 3 and 4, development and validation of a multi-body model that accounts for relative motion of cabinet components is recommended. Cabinets having batteries, power supplies, internal chassis, and cabinet doors with inadequate or flexible restraints are rapidly being infused into shipboard environments. For these cases, cabinet to mount system stiffness ratios of 10:1 are unlikely and rigid body approximations are less accurate. The primary use of a multi-body model would be for post-test analysis after calibration. It is unlikely that parameters of a multi-body model will be sufficiently known to perform pre-test predictions. The calibrated post-test models are useful when baseline cabinet configurations are needed to more accurately assess changes that may occur during the life cycle of the cabinet. These changes may include addition of heavier or lighter subcomponents during equipment upgrades; placement of an identical or modified cabinet in a different shock environment; relocation of mounts; etc. SIMPLE and other 6DOF analysis tools may be modified to include two or more rigid bodies connected by elastic constraints where their stiffness values, weights, and inputs may be varied. Performing post-test calibrations with these variances will help determine the weight configurations and stiffness values that best fit the experimental results. Proposed changes to cabinet configurations may then be evaluated with the calibrated model.

To further investigate question 1, additional research is recommended to determine confidence intervals for uncertain model parameters such as mass moments of inertia and mount load-deflection curves for commonly used mounts. These intervals will provide design constraints for achieving acceptable responses using six degree of freedom (6DOF) analysis tools. They will also improve the efficiency in defining uncertainties used in sensitivity analyses.

Acknowledgement

The first author wishes to acknowledge and thank Glen Sturtevant, the Navy's Smartship Program Manager; George Botto, Smartship Test Director; and Barry Gartman, Shock Test and Analysis Program Manager at Anteon Corporation, Systems Integration Group for supporting this study. The author also wishes to thank Kurt Hartsough, Naval Sea Systems Command (NAVSEA), Carderock, for his technical guidance related to analysis supporting the shock qualification process and Rudolph Scavuzzo, Ph.D., for his instruction in practical shock analysis and identification of relevant literature on this topic area. Shock response spectrum graphs used in this study are from UERDTOOLS, a collection of shock data processing and analysis routines with graphing tools developed by Paul A. Mantz of NAVSEA, Carderock. The material in this manuscript was abstracted from a dissertation developed by the first author for The George Washington University in partial fulfillment of the requirements for the Doctor of Science degree.

References

[1] M. Kikuchi and I. Aiken, An Analytical Hysteresis Model for Elastomeric Seismic Isolation Bearings, *Earthquake Engineering and Structural Dynamics* **26**(2) (February 1997).

[2] Estimation Theory, in: *Probability and Statistics*, M. Spiegel, McGraw-Hill Book Company, New York, 1975, pp. 194–210.

[3] C.M. Richards and R. Singh, Characterization of Rubber Isolator Nonlinearities in the Context of Single- and Multi-Degree of Freedom Experimental Systems, *Journal of Sound and Vibration* **247** (2001), 807–834.

[4] M. Talley, T. Sides and G. Camp, *Underwater Explosion Testing of a Shock-Acoustic Mount and a Tension-Compression Liquid Spring Isolator*, Carderock Division, Naval Surface Warfare Center, Bethesda, MD, Survivability, Structures and Materials Directorate Research and Development Report SSM-66-96-5, 1996.

[5] M. Talley, D. Ingler, M. Riley and G. Messina, *Underwater Explosion Testing of COTS Equipment Items Installed on a Shock Isolated Raft*, Carderock Division, Naval Surface Warfare Center, Bethesda, MD, Survivability, Structures and Materials Directorate Research and Development Report SSM-66-97-5, 1997.

[6] T.L. Carter, *Characterize the Shock Environment of the Medium-Weight Shock Machine*, in 61st Shock and Vibration Symposium Proceedings, October 1990, 60F.

[7] I. Vigness, Elementary Considerations of Shock Spectra, *The Shock and Vibration Bulletin* (34) (December 1964), Part 3.

[8] M. Talley, Six Degree of Freedom Simulation Software for Shock Isolation Mount Predictions and Loading Estimates, *73rd Shock & Vibration Symposium* (2002), U-35.

[9] R.H. Racca, Types and Characteristics of Vibration Isolators, in: *Shock and Vibration Handbook*, 3rd C. Harris, ed., McGraw-Hill Book Company, New York, 1988, pp. 32–1 to 32–28.

[10] D.S. Steinberg, *Vibration Analysis for Electronic Equipment*, 2nd ed., John Wiley & Sons, Inc., New York, 1988, pp. 15 and 276.

[11] C.E. Crede and J.E. Ruzicka, Theory of Vibration Isolation, in: *Shock and Vibration Handbook*, 3rd ed., C. Harris, McGraw-Hill Book Company, New York, 1988, pp. 30–1 to 30–57.

[12] Department of the Navy, Requirements for Shock Tests, H. I. (High Impact) Shipboard Machinery, Equipment, and Systems, Military Specification MIL-S-901D, (17 March 1989).

[13] R.J. Scavuzzo and P. Lam, Decoupling of Undamped Vibration Systems, *Journal of Pressure Vessel technology* **99** (November 1977).

[14] R.E. Newton, Theory of Shock Isolation, in: *Shock and Vibration Handbook*, 3rd ed., C. Harris, McGraw-Hill Book Company, New York, 1988, pp. 31–1 to 31–57.

[15] B.G. Korenev and L.M. Reznikov, Dynamic Vibration Absorbers Theory and Technical Applications, John Wiley & Sons, Inc., New York, 1993.

[16] R.J. Scavuzzo, Shock Qualification by Design Analysis in Practical Shock Analysis and Design, Vol. 1, Vibration Institute, Portsmouth, VA, 1991, pp. 11–1 to 32.

[17] H.L. Hain, J.J. Heintzel and C.J. Leingaug, Application of Isolators, in: *Shock and Vibration Handbook*, 3rd, C. Harris, ed., McGraw-Hill Book Company, New York, 1988, pp. 32–1 to 32–28.

[18] H. Himelblau and R. Sheldon, Vibration of a Resiliently Supported Rigid Body, in: *Shock and Vibration Handbook*, 3rd, C. Harris, ed., McGraw-Hill Book Company, New York, 1988, pp. 3–1 to 3–42.

[19] F.C. Schweppe, Performance of Estimators, in Uncertain Dynamic Systems, Prentice-Hall, Inc., New Jersey, 1973, pp. 382 to 383.

[20] Ventana Systems, Inc., Vensim Standard and Professional DSS Reference Manual Version 3.0, Ventana Systems, Inc., Harvard MA, 1988.

[21] Kinetics of Rigid Bodies in Three Dimensions, in: *Vector Mechanics for Engineers, Statics and Dynamics*, 3rd ed., F. Beer and E. Johnston, Jr., eds, McGraw-Hill Book Company, New York, 1997, pp. 828–874.

[22] Orthogonal Matrices, in: *Mathematical Methods for Physicists*, 3rd ed., G. Arfken, Academic Press, Inc., San Diego, CA, 1985, pp. 191–205.

[23] Deflection of Beams by Integration, in: *Mechanics of Materials*, F. Beer and E. Johnston, Jr., eds, McGraw-Hill Book Company, New York, 1981, pp. 400–426.

[24] Beam Diagrams and Formulas, in: *Manual of Steel Construction*, 8th ed., American Institute of Steel Construction, Inc., Chicago, IL, 1980, pp. 2–111 to 2–116.

[25] S.J. O'Meara, Type I Environmental Vibration Testing of Integrated Ship Controls (ISC) Red Equipment, Date Tested: 12/20/01 to 01/06/02, Hi-Test laboratories, Inc. Report No. 1024, April 2002.

[26] S.J. O'Meara, Heavyweight High Impact Shock Testing of Integrated Ship Controls (ISC) Equipment on the White Barge, Date Tested: 12/21/01 to 01/14/02, Hi-Test laboratories, Inc. Report No. 1022, April, 2002.

[27] S.J. O'Meara, Heavyweight High Impact Shock Testing of Integrated Ship Controls (ISC) Equipment on the Blue Barge, Date Tested: 01/26/02 to 01/29/02, Hi-Test laboratories, Inc. Report No. 1028, April, 2002.

[28] S.J. O'Meara, Heavyweight High Impact Shock Testing of Integrated Ship Controls (ISC) Equipment on the Silver Barge, Date Tested: 05/01/02 to 05/03/02, Hi-Test laboratories, Inc. Report No. 1050, August, 2002.

[29] Dynamic Testing Inc., June 2001, High Impact (H.I.) Heavyweight Shock Test Report for Shock Qualification of the Integrated Condition Assessment System (ICAS) Units, DTI Report No. 474.
[30] E.W. Swokowski, Numerical Integration, in: *Calculus With Analytic Geometry*, Prendle, Weber & Schmidt, Boston, MA, 1979, pp. 260.
[31] G. Burgess, Extension of Fatigue Model for Product Shock Fragility Used in Package Design, *Journal of Testing and Evaluation, JETVA* **28**(2) (March 2000), 116 to 120.
[32] S.J. O'Meara, Type I Environmental Vibration Testing of Integrated Ship Controls (ISC) White Equipment, Date Tested: 12/10/01 to 12/13/01, Hi-Test laboratories, Inc. Report No. 1023, April, 2002.